Inorganic Chemistry

Article

pubs.acs.org/IC

Use of Metalloligands [CuL] (H_2L = Salen Type Di-Schiff Bases) in the Formation of Heterobimetallic Copper(II)-Uranyl Complexes: Photophysical Investigations, Structural Variations, and Theoretical Calculations

Soumavo Ghosh,[†] Saptarshi Biswas,[†] Antonio Bauzá,[‡] Miquel Barceló-Oliver,[‡] Antonio Frontera,*[,‡] and Ashutosh Ghosh*[,†]

[†]Department of Chemistry, University College of Science, University of Calcutta, 92, A.P.C. Road, Kolkata-700 009, India

[‡]Departament de Química, Universitat de les Illes Balears, Crta. de Valldemossa km 7.5, 07122 Palma de Mallorca (Baleares), Spain

Supporting Information

ABSTRACT: Five heterobimetallic copper(II)−uranium(VI) complexes $[(CuL^1)UO_2(NO_3)_2]$ (**1**), $[\{CuL^1(CH_3CN)\}UO_2(NO_3)_2]$ (**2**), $[\{CuL^1(CH_3COCH_3)\}UO_2(NO_3)_2]$ (**3**), $[\{CuL^2(CH_3CN)\}UO_2(NO_3)_2]$(**4**), and $[\{CuL^2(CH_3COCH_3)\}UO_2(NO_3)_2][\{CuL^2\}UO_2(NO_3)_2]$ (**5**) have been synthesized by reacting the Cu(II)-derived metalloligands $[CuL^1]$ and $[CuL^2]$ (where, H_2L^1 = *N*,*N*′-bis(α-methylsalicylidene)-1,3-propanediamine and H_2L^2 = *N*,*N*′-bis(salicylidene)-1,3-propanediamine) with $UO_2(NO_3)_2{\cdot}6H_2O$ in 1:1 ratio by varying the reaction temperature and solvents. Absorption and fluorescence quenching experiments (steady-state and time-resolved) indicate the formation of 1:1 ground-state charge transfer copper(II)−uranium(VI) complexes in solution. X-ray single-crystal structure reveals that each complex contains diphenoxido bridged Cu(II)−U(VI) dinuclear core with two chelated nitrato coligands. The complexes are solvated (acetonitrile or acetone) in the axial position of the Cu(II) in different manner or desolvated. The supramolecular interactions that depend upon the co-ordinating metalloligands seem to control the solvation. In complexes **2** and **3** a rare $NO_3^-\cdots NO_3^-$ weak interaction plays an important role in forming supramolecular network whereas an uncommon $U{=}O\cdots NO_3^-$ weak interaction helps to self-assemble heterobinuclear units in complex **5**. The significance of the noncovalent interactions in terms of energies and geometries has been analyzed using theoretical calculations.

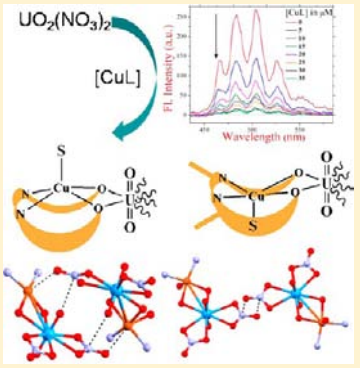

INTRODUCTION

One of the recent trends in co-ordination chemistry is to explore new types of molecular architectures using relatively less common metal ions. The f-block metals especially come into this scenario as they have shown potentiality toward multifunctional materials in terms of magnetic and optical properties.[1] In contrast to recently developed copious novel multifunctional heteronuclear 3d-4f molecular compounds and co-ordination polymers, only a few heterometallic 3d-5f complexes are reported. These 3d-5f complexes are derived mainly from uranium in different oxidation states by using various types of ligands, for example, phosphonates, hexadentate bicompartmental N_2O_4 Schiff base metalloligands, etc.[2] The compounds containing lower valence uranium ($U^{III/IV/V}$) have been synthesized mostly to explore their interesting magnetic properties.[3] On the other hand, the naturally occurring uranyl compounds which are known for their interesting photophysical properties for centuries and have immense importance in terms of environmental, geological, or bioassay fields[4] are scarcely explored to make photo responsive systems using interactions between transition metal complexes and uranyl ions.[5]

The hexadentate bicompartmental ligands have been found to be very convenient to create heterometallic complexes including 3d-4f metal ions.[6] In recent years the use of monocompartmental chelates derived from tetradentate salen type Schiff bases (salen = *N*,*N*′-bis(salicylidene)-ethylenediamine) is also gaining popularity.[7] The oxygen atoms of the neutral Cu(II) and Ni(II)-chelate of such ligands can coordinate to a second metal ion providing a facile way for the synthesis of bi-, tri-, tetra-, or polynuclear heterometallic complexes in which the second metal ion is a s-block, p-block, d-block, or 4f-block cation.[8] However, to date these chelates have not been used to synthesize heterometallic 3d-5f complexes. As actinyls are hard acids with a strong oxophilic character and prefer high coordination numbers (five, six or seven) around the equatorial plane, they are expected to be incorporated easily by these monocompartmental chelates.[9]

UO_2^{2+} containing minerals and compounds display vibrationally resolved ligand-to-metal charge transfer (LMCT) emission around 520 nm in solution and in the solid state.

Received: February 18, 2013
Published: June 20, 2013

   dx.doi.org/10.1021/ic400422d | *Inorg. Chem.* 2013, 52, 7508−7523

This optical property has been exploited to study the interaction with other molecules.[10] On the other hand, the interaction of Cu^{2+} with various fluorophores has been investigated in detail as it is proved to be a very efficient quencher for fluorescence active materials.[11] Free Cu^{2+} is also well-known to quench efficiently the fluorescence of uranyl ion by interacting with its excited state.[12] However, till now there is no evidence whether Cu(II) based salen type Schiff base derived metalloligands have such quenching properties. We would like to explore the interaction of uranyl ion with [CuL] (where H_2L = salen type Schiff base) using the former as luminescence probe[13] and also to crystallize the product and investigate them by single crystal X-ray crystallography.

In the present work, we use two "metalloligands" [CuL^1] and [CuL^2], where H_2L^1 = *N*,*N*′-bis(α-methylsalicylidene)-1,3-propanediamine and H_2L^2 = *N*,*N*′-bis(salicylidene)-1,3-propanediamine to study the complex formation with uranyl nitrate. The formation of the heterodinuclear ground state charge transfer complex in solution has been characterized by steady state and time-resolved fluorescence quenching experiments using the uranyl as a luminescence probe. The structural analyses reveal that both [CuL^1] and [CuL^2] form a 1:1 adduct with $UO_2(NO_3)_2$ which can be crystallized either in solvated or in desolvated form. Interestingly, in the solvated complexes the solvent molecules coordinate to the axial position of the Cu(II) via the concave or convex side of the bowl shaped coordinated Schiff base depending upon the ligands. These differences have been rationalized by using density functional theory (DFT) calculations. We also perform an energetic study to analyze the importance of the weak noncovalent forces for less common $NO_3^-\cdots NO_3^-$, and $U{=}O\cdots NO_3^-$ interactions as well as for more common C−H···O and C−H/π interactions that influence the crystal packing. To the best of our knowledge, this is the first report investigating the adduct formations of uranyl ion with Cu(II)-salen type "metalloligands" with the help of absorption and emission spectra, single crystal X-ray analysis, and theoretical study.

EXPERIMENTAL SECTION

Starting Materials. The salicylaldehyde, 2-hydroxyacetophenone, and 1,3-propanediamine were purchased from Lancaster and were of reagent grade. They were used without further purification. Reagent grade $UO_2(NO_3)_2{\cdot}6H_2O$ was purchased from Aldrich.

Caution! *Perchlorate salts of metal complexes with organic ligands are potentially explosive. Only a small amount of material should be prepared, and it should be handled with care. All uranyl compounds are toxic when ingested, and any contact with the skin should also be avoided because of its mild radioactivity.*

Synthesis of the Schiff Base Ligands H_2L^1, H_2L^2 and Ligand Complexes [CuL^1], [CuL^2]. Two di-Schiff-base ligands, H_2L^1 and H_2L^2, were prepared by standard methods.[14] Briefly, 5 mmol of 1,3-propanediamine (0.42 mL) were mixed with 10 mmol of the required carbonyl compound (2-hydroxyacetophenone (1.2 mL) or salicylaldehyde (1.0 mL) respectively) in methanol (20 mL). The resulting solutions were refluxed for about 2 h and allowed to cool. The yellow colored methanolic solutions were used directly for complex formation. To a methanolic solution (20 mL) of $Cu(ClO_4)_2{\cdot}6H_2O$ (1.852 g, 5 mmol), a methanolic solution of H_2L^1 or H_2L^2 (5 mmol, 10 mL) and triethyl amine (1.4 mL, 10 mmol) were added to prepare the respective precursor "metalloligands" [CuL^1] and [CuL^2], as reported earlier.[14]

Synthesis of Complex [(CuL^1)$UO_2(NO_3)_2$] (1). The "metalloligand" [CuL^1] (14.8 mg, 0.04 mmol) was dissolved in acetonitrile (5 mL) and to it a solution of $UO_2(NO_3)_2{\cdot}6H_2O$ (20.0 mg, 0.04 mmol in 5 mL of acetonitrile) was added, stirred for 5 min and then allowed to stand overnight at room temperature when reddish microcrystalline compound deposited at the bottom of the vessel. This compound was isolated by filtration and redissolved in 5 mL of acetone by warming, and the solution was kept in a long tube for slow evaporation. X-ray quality single crystals of complex **1** appeared after about 15 days.

Compound ***1***. Yield: 22.7 mg. (74%). $C_{19}H_{20}CuN_4O_{10}U$ (765.96): calcd. C 29.79, H 2.63, N 7.31; Found C 29.91, H 2.77, N 7.04. UV/vis: λ_{max} (MeCN, absorbance) = 663, 317, 261, and 225 nm; λ_{max} (solid, reflectance) = 585 and 368 nm. IR: ν(C═N) = 1598.6 cm^{-1}, ν(U═O) = 922.6 cm^{-1}, $\nu(NO_3^-)$ = 1482.6 cm^{-1} (ν_1), 1296.9 cm^{-1} (ν_2), 1025.7 cm^{-1} (ν_3).

Synthesis of Complexes [{$CuL^1(CH_3CN)$}$UO_2(NO_3)_2$] (2) and [{$CuL^1(CH_3COCH_3)$}$UO_2(NO_3)_2$] (3). The "metalloligand" [CuL^1] (14.8 mg, 0.04 mmol) was dissolved in acetonitrile (2 mL), in a 5 mL vial and kept in a refrigerator for about 1 h to cool the solution. To this solution, a cold solution of $UO_2(NO_3)_2{\cdot}6H_2O$ (20.0 mg, 0.04 mmol in 2 mL of acetonitrile) was added, stirred to mix, and the mixture was brought back in the refrigerator within 1 min. The solution was allowed to stand overnight in the refrigerator when brown X-ray quality single crystals of complex **2** appeared. Complex **3** was obtained by following a similar procedure to that of **2**, but acetone was used as solvent instead of acetonitrile.

Complex ***2***. Yield: 20.0 mg. (62%). $C_{21}H_{23}CuN_5O_{10}U$ (807.02): calcd. C 31.25, H 2.87, N 8.68; Found C 30.98, H 2.88, N 8.77. UV/vis: λ_{max} (MeCN, absorbance) = 663, 317, 261, and 225 nm; λ_{max} (solid, reflectance) = 645 and 362 nm. IR: ν(C═N) = 1598.2 cm^{-1}, ν(U═O) = 927.6 cm^{-1}, $\nu(NO_3^-)$ = 1524.6 cm^{-1} (ν_1), 1293.6 cm^{-1} (ν_2), 1027.9 cm^{-1} (ν_3),

Complex ***3***. Yield: 21.4 mg. (65%). $C_{22}H_{26}CuN_4O_{11}U$ (824.05): calcd. C 32.07, H 3.18, N 6.80; Found C 32.31, H 3.27, N 6.67. UV/vis: λ_{max} (acetone, absorbance) = 657, 312, 255, 223 nm; λ_{max} (solid, reflectance) = 640 and 372 nm. IR: ν(C═N) 1597.9 cm^{-1}, ν(C═O) = 1691.8 cm^{-1}, ν(U═O) = 926.1 cm^{-1}, $\nu(NO_3^-)$ = 1526.2 cm^{-1} (ν_1), 1291.4 cm^{-1} (ν_2), 1027.3 cm^{-1} (ν_3).

Synthesis of Complex [{$CuL^2(CH_3CN)$}$UO_2(NO_3)_2$] (4). The "metalloligand" [CuL^2] (13.8 mg, 0.04 mmol) was dissolved in acetonitrile (5 mL) and to it a solution of $UO_2(NO_3)_2{\cdot}6H_2O$ (20.0 mg, 0.04 mmol in 5 mL) was added, stirred for 5 min, filtered and then allowed to stand at room temperature for slow evaporation. A greenish microcrystalline compound started to deposit at the bottom of the vessel after a few hours. The compound was redissolved in acetonitrile (10 mL) by warming, filtered, and the solution was kept at open atmosphere. Dark green X-ray quality single crystals of complex **4** appeared within 2 days.

Complex ***4***. Yield: 22.1 mg. (71%). $C_{19}H_{19}CuN_5O_{10}U$ (778.97): calcd. C 29.30, H 2.46, N 8.99; Found C 29.51, H 2.57, N 8.87. UV/vis: λ_{max} (MeCN, absorbance) = 630, 329, 269, and 229 nm; λ_{max} (solid, reflectance) = 647 and 358 nm. IR: ν(C═N) = 1637.1 cm^{-1}, ν(U═O) = 933.8 cm^{-1}, $\nu(NO_3^-)$ = 1526.3 cm^{-1} (ν_1), 1278.3 cm^{-1} (ν_2), 1024.6 cm^{-1} (ν_3).

Synthesis of Complex [{$CuL^2(CH_3COCH_3)$}$UO_2(NO_3)_2$][{CuL^2}-$UO_2(NO_3)_2$] (5). The "metalloligand" [CuL^2] (13.8 mg, 0.04 mmol) was dissolved in 1:1 acetone-methanol mixture (v/v, 2 mL) and to it a 2 mL solution of $UO_2(NO_3)_2{\cdot}6H_2O$ (20.0 mg, 0.04 mmol) in the same solvent mixture was added, stirred to mix, transferred to a 5 mL vial, sealed and kept at room temperature. After one week brown X-ray quality single crystals of complex **5** appeared as the solvent evaporated slowly.

Complex ***5***. Yield: 17.6 mg. (57%). $C_{37}H_{38}Cu_2N_8O_{21}U_2$ (1533.92): calcd. C 28.97, H 2.50, N 7.31; Found C 28.71, H 2.48, N 7.47. UV/vis: λ_{max} (Acetone, absorbance) = 631, 324, 265, and 226 nm; λ_{max} (solid, reflectance) = 617 and 356 nm. IR: ν(C═N) 1628.5 cm^{-1}, ν(C═O) = 1698.1 cm^{-1}, ν(U═O) = 928.8 cm^{-1}, $\nu(NO_3^-)$ = 1479.2 cm^{-1} (ν_1), 1276.2 cm^{-1} (ν_2), 1033.7 cm^{-1} (ν_3).

Physical Measurements. Elemental analyses (C, H, and N) were performed using a Perkin-Elmer 2400 series II CHN analyzer. IR spectra in KBr pellets (4000−500 cm^{-1}) were recorded using a Perkin-Elmer RXI FT- IR spectrophotometer. Thermal analyses (TG-DTA) were carried out on a Mettler Toledo TGA/SDTA 851 thermal analyzer in a dynamic atmosphere of N_2 (flow rate 50 cm^3 min^{-1}). The

dx.doi.org/10.1021/ic400422d | *Inorg. Chem.* 2013, 52, 7508−7523

Table 1. Crystal Data and Refinement Details of the Complexes 1−5

	1	2	3	4	5
formula	$C_{19}H_{20}CuN_4O_{10}U$	$C_{21}H_{23}CuN_5O_{10}U$	$C_{22}H_{26}CuN_4O_{11}U$	$C_{19}H_{19}CuN_5O_{10}U$	$C_{37}H_{38}Cu_2N_8O_{21}U_2$
formula wt.	765.96	807.02	824.05	778.97	1533.92
crystal sys.	orthorhombic	orthorhombic	orthorhombic	monoclinic	monoclinic
space gr.	*Pnma*	$P2_12_12_1$	$P2_12_12_1$	$P12_1/m1$	$P2_1/n$
a /Å	18.525(2)	11.0318(12)	11.155(4)	9.2815(4)	18.635(5)
b /Å	20.136(2)	12.4097(14)	12.610(5)	15.4392(7)	25.264(5)
c /Å	6.1995(7)	19.319(2)	18.864(7)	9.3057(4)	24.446(5)
β /deg	90	90	90	116.012(2)	125.880(13)
V /Å^3	2312.5(4)	2644.8(5)	2653.5(17)	1198.42(9)	9325(4)
Z	4	4	4	2	8
D_c/g cm^{-3}	2.200	2.027	2.063	2.159	2.185
μ/mm^{-1}	7.976	6.981	6.963	7.699	7.908
R(int)	0.0884	0.0424	0.0783	0.0446	0.0735
unique data	2084	4390	4611	2557	15826
data with $I > 2\sigma(I)$	1686	4065	3653	2259	9963
R1 ($I > 2\sigma(I)$)	0.0950	0.0279	0.0568	0.0249	0.0650
*w*R2 ($I > 2\sigma(I)$)	0.2702	0.0595	0.1296	0.0590	0.1585
GOF on F^2	1.161	1.011	1.003	1.022	1.046

samples were heated in an alumina crucible at a rate of 10 °C min^{-1} up to 600 °C. All solutions were prepared in spectroscopic grade solvents. At least seven experimental data points were made up for B−H plots and quenching experiments. Electronic spectra were recorded in acetone and acetonitrile (800−200 nm) in a 1 cm optical glass cuvette as well as in solid state (800−300 nm) in a Hitachi U-3501 spectrophotometer using appropriate set up. All the steady-state and time-resolved measurements were performed at room temperature 25 ± 2 °C under aerial condition. The uranyl concentration (as nitrate) was usually 3 mM. The steady-state fluorescence emission spectra were recorded using a PerkinElmer LS-55 spectrofluorimeter after proper background correction with individual solvents within the range 435−650 nm using 424 nm excitation wavelength in quartz cells with 1 cm path length. When the metalloligands were used to quench $*UO_2^{2+}$, the metalloligand concentration was varied from 5 to 35 μM to prevent any self-aggregation of the quencher. Optical density correction was done when needed. Both excitation and emission slit widths are kept at 5 nm. Normalized fluorescence intensity (I_0/I) (where I_0 and I are the measured fluorescence intensities in absence and presence of quencher) is used as a function for steady state Stern Volmer analysis. The decay times of the $UO_2(NO_3)_2$ in the microseconds region were also acquired by phosphorescence decay mode in QM-30 fluorimeter from PTI, U.S.A., using a gated detection system having start and end window time of 0 and 6000 μs, respectively, in which emission intensity was measured as a function of time at 505 nm using λ_{ex} of 424 nm. The decay parameters were recovered using a nonlinear iterative fitting procedure based on the Marquardt algorithm.[15] All calculations were done by Origin 7.0 software.

Crystal Data Collection and Refinement. Suitable single crystals of all the complexes were mounted on a Bruker-AXS SMART APEX II diffractometer equipped with a graphite monochromator and MoK_α (λ = 0.71073 Å) radiation. The crystals were positioned at 60 mm from the CCD. A total of 360 frames were measured with a counting time of 10 s. The structures were solved using Patterson method by using the SHELXS 97 program. Subsequent difference Fourier synthesis and least-squares refinement revealed the positions of the remaining non-hydrogen atoms. Non-hydrogen atoms were refined with independent anisotropic displacement parameters. Hydrogen atoms were placed in idealized positions and refined riding on their parent atoms. Absorption corrections were carried out using the SADABS program.[16] All calculations were carried out using SHELXS 97,[17] SHELXL 97,[18] PLATON 99,[19] ORTEP-32,[20] and WinGX system Ver-1.64.[21] Data collection with structure refinement parameters and bond parameters for the five complexes are given in Table 1 and Supporting Information, Tables S1−S4 respectively.

Computational Methods. The energies of all complexes included in this study were computed at the BP86-D3/def2-TZVPD level of theory using the crystallographic coordinates within the program TURBOMOLE version 6.4.[22] The interaction energies were calculated with correction for the basis set superposition error (BSSE) by using the Boys−Bernardi counterpoise technique.[23] For the calculations we have used the BP86 functional with the latest available correction for dispersion (D3).[24]

RESULTS AND DISCUSSION

Syntheses, IR Spectroscopy and Thermal Analysis of the Complexes. The Schiff-base ligands (H_2L^1 and H_2L^2) and their Cu(II) complexes ([CuL^1] and [CuL^2]) were synthesized using the reported procedures.[14] Reaction of [CuL^1] with uranyl nitrate in acetonitrile medium at room temperature (25−30 °C) produces a red microcrystalline compound which on recrystallization from acetone yields red single crystals of complex **1**, [(CuL^1)$UO_2(NO_3)_2$]. However, when the same reaction is carried out at low temperature (~5 °C) brown single crystals of complex **2**, [{$CuL^1(CH_3CN)$}$UO_2(NO_3)_2$], result from the acetonitrile solution. The difference between complexes **1** and **2** is that Cu(II) is square planar in **1** whereas an acetonitrile solvent molecule is coordinated to the axial position of Cu(II) center in **2**. The reaction has also been carried out in acetone medium, and it is found that at low temperature an acetone molecule coordinates to the Cu(II) center to produce complex **3**, [{$CuL^1(CH_3COCH_3)$}-$UO_2(NO_3)_2$], which geometrically resembles complex **2**. Therefore, coordination of solvent molecules to the Cu(II) center depends upon the temperature of the reaction mixture but not on polarity or Lewis basicity of the coordinating solvent molecules used here.

On the other hand, in case of the metalloligand [CuL^2], complex **4** [{$CuL^2(CH_3CN)$}$UO_2(NO_3)_2$] having penta-coordinated Cu(II) with axially coordinated solvent molecules resulted at room temperature. However, the geometry does not resemble complexes **2** and **3**. The difference lies in the direction of axial coordination of solvents to Cu(II) with respect to the Schiff bases H_2L^1 or H_2L^2 which adopt a shape of a bowl around the Cu(II); the solvents coordinate through the concave part of the bowl for complexes **2** and **3** whereas for complex **4** through the convex part. We failed to obtain single

dx.doi.org/10.1021/ic400422d | Inorg. Chem. 2013, 52, 7508−7523

Scheme 1. Formation of Complexes 1−5

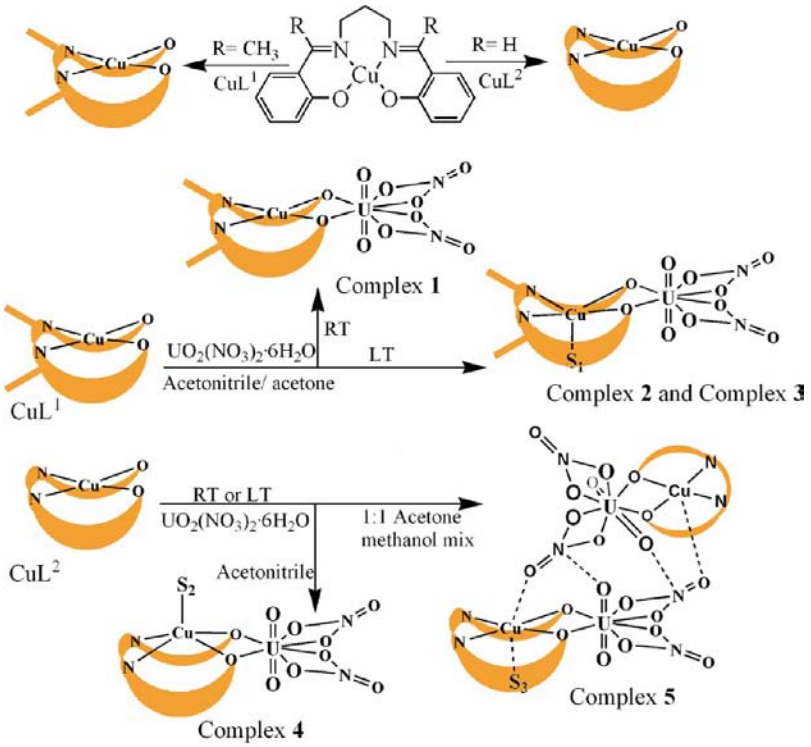

S_1=Acetonitrile for complex **2** and acetone for complex **3**, S_2=Acetonitrile, and S_3=Acetone,
LT = Low temperature (0–5°C), RT = Room temperature (25–30°C)

crystals of this compound from acetone only but succeeded to get crystals of complex **5** ($[\{CuL^2(CH_3COCH_3)\}UO_2(NO_3)_2][\{CuL^2\}UO_2(NO_3)_2]$ from a 1:1 acetone-methanol mixture (v/v) (Scheme 1). In the structure of **5** both square planar and square pyramidal Cu(II) centers are present. The geometry of square pyramidal Cu(II) resembles complexes **2** or **3**. Interestingly, for both **4** and **5**, the crystals obtained at room temperature and at low temperature are identical.

Besides elemental analyses, all the complexes were initially characterized by IR spectra. The precursor metalloligands $[CuL^1]$ and $[CuL^2]$ are neutral and do not have any counteranion whereas all five complexes contain IR active uranyl and nitrato moieties. The nitrato anion shows its characteristic bands for bidentate chelation in each compound.[25] The asymmetric vibration of the O═U═O moiety appears in the range of 923−928 cm^{-1} for complexes **1**−**3** whereas it lies between 929−934 cm^{-1} for complexes **4** and **5**. In all complexes, a strong and sharp band due to the azomethine ν(C═N) group of the Schiff base appears at 1598−1599 for $[CuL^1]$ and 1628−1637 cm^{-1} for $[CuL^2]$, respectively.

The thermo-gravimetric analyses were carried out in a N_2 atmosphere on powder samples of complexes **1**−**5**. Complex **1** does not show any mass loss till the temperature is raised to 250 °C corroborating the absence of any solvent molecule in the structure (Supporting Information, Figure S1A). On the other hand, both complexes **2** and **3**, that is, the solvated forms of complex **1** show endothermic weight loss of 4.1% and 7.0%, in the temperature ranges 139−185 °C and 137−201 °C owing to the loss of acetonitrile (calc. 5.1%) and acetone (calc. 7.0%) molecules, respectively, followed by the pyrolytic ligand degradation like **1** (Supporting Information, Figures S1B and S1C). Similarly complexes **4** and **5** show the steps for the loss of solvents acetonitrile (obs.: 3.7%, calc. 4.0%, between 88 and 168 °C) for **4** and acetone (obs.: 2.7%, calc. 3.8%, between 89 and 156 °C) for **5** (Supporting Information, Figures S1D and S1E). On further heating both the complexes start to decompose at about 250 °C like **1**−**3**.

■ ELECTRONIC SPECTROSCOPY

Absorption Spectroscopy. The interactions of uranyl ion with metalloligands ($[CuL^1]$ and $[CuL^2]$) in acetonitrile solutions are characterized by UV−vis absorption and fluorescence spectroscopy. The electronic absorption spectrum of $[CuL^1]$ exhibits two bands at 360 and 580 nm in acetonitrile whereas the same for $[CuL^2]$ appears at 365 and 607 nm (Supporting Information, Figure S2A and S2B, respectively). These bands are characterized as ligand-to-metal charge transfer (LMCT) and d-d transition of the metalloligands, respectively.[26] Because of complexation with the uranyl center, the d-d transition band of the metalloligands exhibits a bathochromic shift to 663 and 630 nm for $[CuL^1]$ and $[CuL^2]$, respectively, in acetonitrile. Similarly, the LMCT band exerts an expected hypsochromic shift to 317 and 329 nm for $[CuL^1]$ and $[CuL^2]$ respectively (Supporting Information, Figure S2A and S2B, respectively). This is also observed for the solid state UV−vis spectrum of the complexes where the d-d transition bands of the metalloligands exhibit bathochromic shifts for complexes **2** (645 nm), **3** (640 nm) and **4** (647 nm), **5** (617 nm) with respect to the free $[CuL^1]$ (620 nm) and $[CuL^2]$ (595 nm), respectively (Supporting Information, Figure S2C and S2D, respectively) in conformity with the square pyramidal Cu(II)

dx.doi.org/10.1021/ic400422d | Inorg. Chem. 2013, 52, 7508−7523

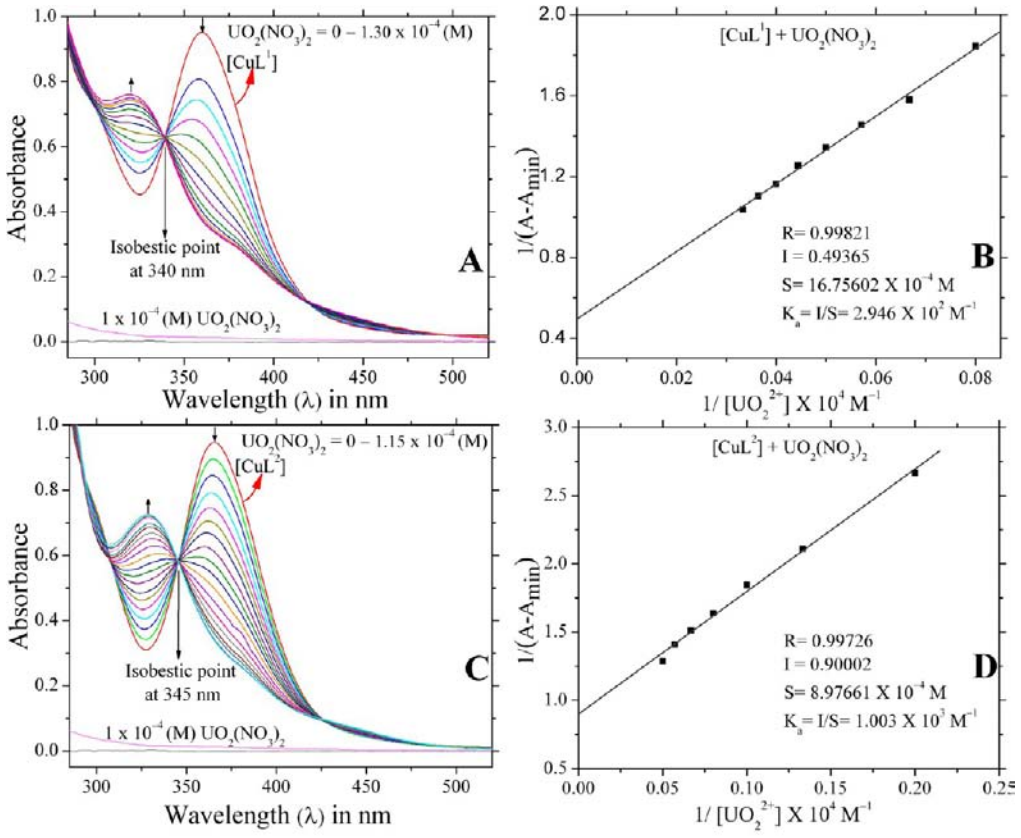

Figure 1. Upper panel for $[CuL^1]$ (1A, 1B), lower panel for $[CuL^2]$ (1C, 1D), left panel for spectrophotometric titration of the fixed concentration of 1×10^{-4} M of the corresponding metalloligands (1A, 1C) by $UO_2(NO_3)_2$, right panel for B−H plot for the respective complexes (1B, 1D) using a fixed concentration of 0.40×10^{-4} M of individual metalloligands and varying concentration of 0.5−2.0 mM for $UO_2(NO_3)_2$.

centers in the solid state structure. For complex **1** a shoulder near 585 nm is observed due to the d-d transition of the square planar Cu(II) center. The electronic spectral data for complexes **2**, **3**, **4**, and **5** are found to be almost similar in both solution and solid state indicating that the complexes retain their solid state structures in solutions.

The existence of isosbestic points in the spectrum is a useful guide to confirm that the reacting species are in equilibrium.[27] Upon gradual addition of $UO_2(NO_3)_2$ solution (1 mM) to a solution of the respective metalloligands (2 mL, 0.1 mM), the bands of $[CuL^1]$ and $[CuL^2]$ at 360 and 365 nm respectively show significant lowering of absorption intensity. Notably, both the metalloligands $[CuL^1]$ and $[CuL^2]$ display a new absorption band centered at 317 and 329 nm, respectively, with increasing intensity which is attributed to the formation of ground-state charge-transfer complexes (Figure 1A and 1C). Appearances of well anchored isosbestic points centered at λ = 340 nm for $[CuL^1]$ and λ = 345 nm for $[CuL^2]$ are consistent with the existence of an equilibrium between metalloligand $[CuL^1]$ or $[CuL^2]$ and uranyl complexes in solutions. The stoichiometry and association constants of these newly formed ground-state charge-transfer complexes can be obtained from the intercept and slope of the Benesi−Hildebrand plot where the increase of absorbance is measured as a function of varied analytical concentration of uranyl salt. The metalloligands' concentration are maintained at least 10 times lower than the lowest concentration of $UO_2(NO_3)_2$ so that the unbound state of these ligands does not contribute appreciably to the overall signal (<5%).[28] Furthermore, a linear relationship is obtained (Figure 1B and 1D) from the absorption titration profiles (40 μM for individual metalloligands and 0.5−2.0 mM for $UO_2(NO_3)_2$ in acetonitrile) for the plots (R = 0.9982 for $[CuL^1]$ and 0.9973 for $[CuL^2]$) of measured $[1/(A - A_{min})]$ at 317 nm for $[CuL^1]$ and 330 nm for $[CuL^2]$ as a function of $1/[UO_2(NO_3)_2]$ using the Benesi−Hildebrand expression,[28] which indicates a ∼1:1 stoichiometry for the complexes formed between metalloligand $[CuL^1]$ or $[CuL^2]$ and $UO_2(NO_3)_2$ in solution. Calculated association constants obtained from the ratio of the intercept to the slope for $[CuL^1]$ and $[CuL^2]$ are K_a = 2.946×10^2 and 1.003×10^3 M^{-1} respectively. Thus from these UV−vis studies, formation of a new 1:1 ground state complex of uranyl with each of the [CuL] is established. However, as uranyl ion is known to form a 1:1 adduct with the Schiff base ligand itself,[29] the above observations are insufficient to establish definitely that the expected Cu-UO_2 hetero-dinuclear complex is formed. Therefore, fluorescence spectroscopic analyses have been undertaken.

EMISSION SPECTROSCOPY

I. Steady State and Time-Resolved Fluorescence Studies of $UO_2(NO_3)_2$. The fluorescence spectrum of 2×10^{-3} M $UO_2(NO_3)_2$ in acetonitrile (excitation wavelength (λ_{ex}) at 424 nm) shows vibronically resolved structured emission bands at 466, 483, 505 (λ_{em}), 525, and 550 nm of this fluorescence probe which correspond to electronic and vibronic transitions $S_{11}-S_{00}$ and $S_{10}-S_{0\nu}$ (ν = 0−4)[2b,30] (Supporting Information, Figure S3A). As molecular oxygen is not involved in depopulating the uranyl excited state,[31] all experiments have

dx.doi.org/10.1021/ic400422d | Inorg. Chem. 2013, 52, 7508−7523

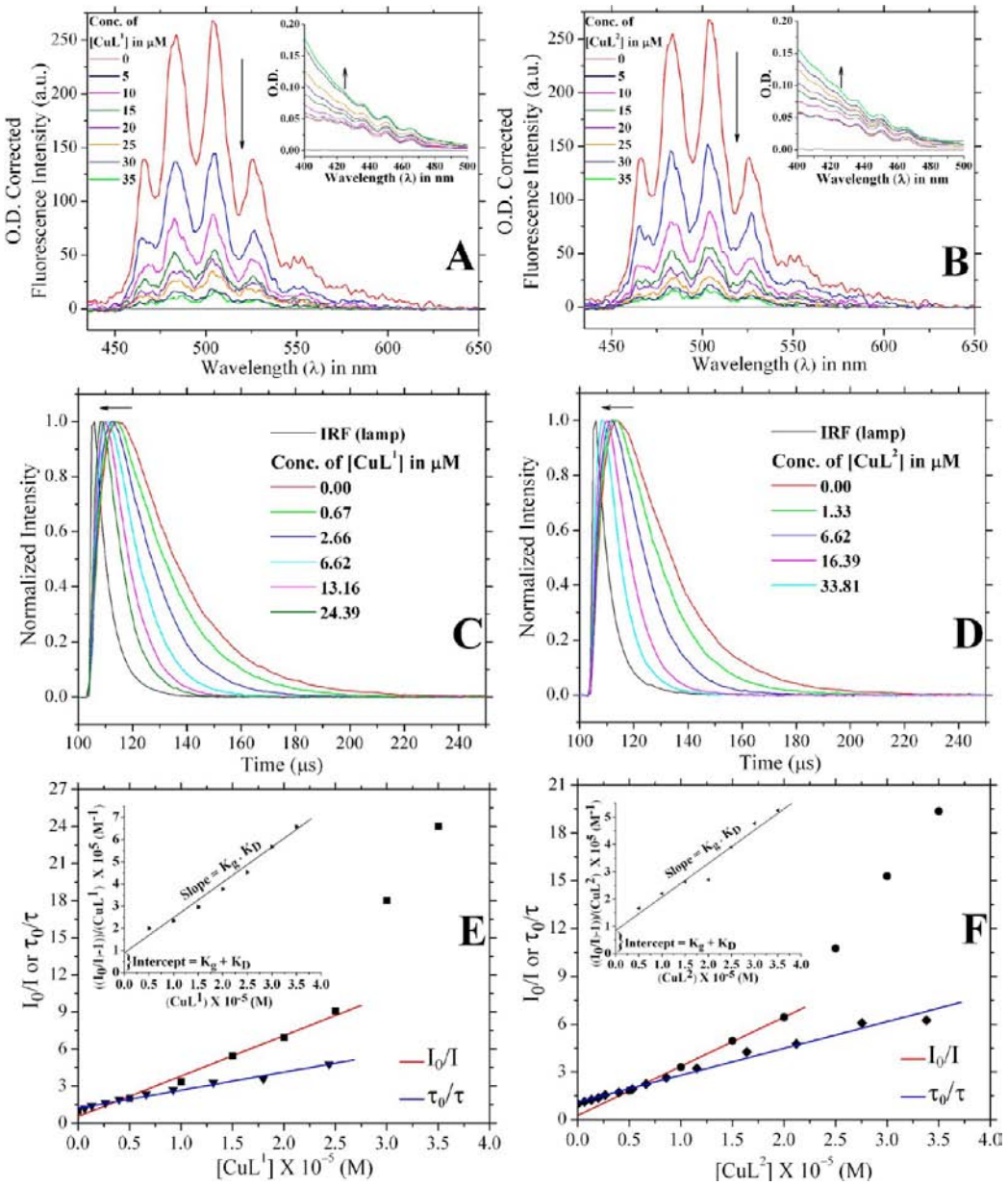

Figure 2. Right panel for [CuL^1] (2A, 2C, 2E), left panel for [CuL^2] (2B, 2D, 2F), top panel for steady state fluorescence quenching titration (2A, 2B) and middle panel for time-resolved fluorescence quenching titration (2C, 2D) of $UO_2(NO_3)_2$ (3.0 mM) by the corresponding metalloligands and bottom panel for S−V plots for the respective metalloligands (2E, 2F).

been performed in aerial atmosphere. The excited state average lifetime (τ_{av}) of $UO_2(NO_3)_2$ with a single exponential decay profile was found to be 2.3 μs in acetone as was reported earlier[32] whereas in acetonitrile the τ_{av} was found to be relatively longer (20.0 μs). The free metalloligands as well as their respective uranyl complexes are nonfluorescent (exciting at their corresponding λ_{max}) in acetonitrile (Supporting Information, Figure S3B). Moreover in solutions the uranyl excited states are known to be collisionally quenched by most of the transition metals having unpaired d-electrons which effectively depopulate both excited singlet and triplet states of the fluorophore.[33] This allows us to look for more insight into the interaction of $UO_2(NO_3)_2$ with the metalloligands [CuL^1] and [CuL^2] using them as a suitable quencher of uranyl fluorescence in solution.

II. Steady State and Time-Resolved Fluorescence Quenching Studies of $UO_2(NO_3)_2$ Using [CuL^1] or [CuL^2]. The UV absorption at λ_{ex} (424 nm) and steady-state fluorescence spectra of $UO_2(NO_3)_2$ in acetonitrile were recorded in the absence and in the presence of different concentrations of quencher, that is, the metalloligands. The typical absorption and fluorescence spectra in acetonitrile in the presence of increasing concentration (0.0−3.5 × 10^{-5} M) of individual metalloligands are shown in Figure 2A and 2B. From the spectra, the following observations are made: (i) the fluorescence intensity of $UO_2(NO_3)_2$ decreases with the increasing concentration of quencher, (ii) the shape and band maxima of absorption and fluorescence spectra remain the same, and (iii) no other emission band of the fluorophore toward longer wavelength appears. These observations suggest that the fluorophore−quencher interaction does not alter the

dx.doi.org/10.1021/ic400422d | Inorg. Chem. 2013, 52, 7508−7523

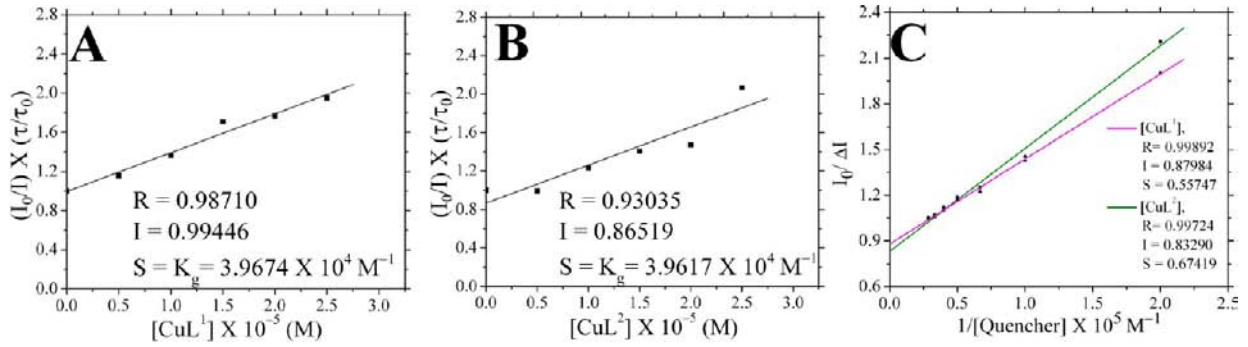

Figure 3. (A) Static quenching plot for [CuL^1]. (B) Static quenching plot for [CuL^2]. (C) Fluorophore accessibility plot for both [CuL^1] and [CuL^2].

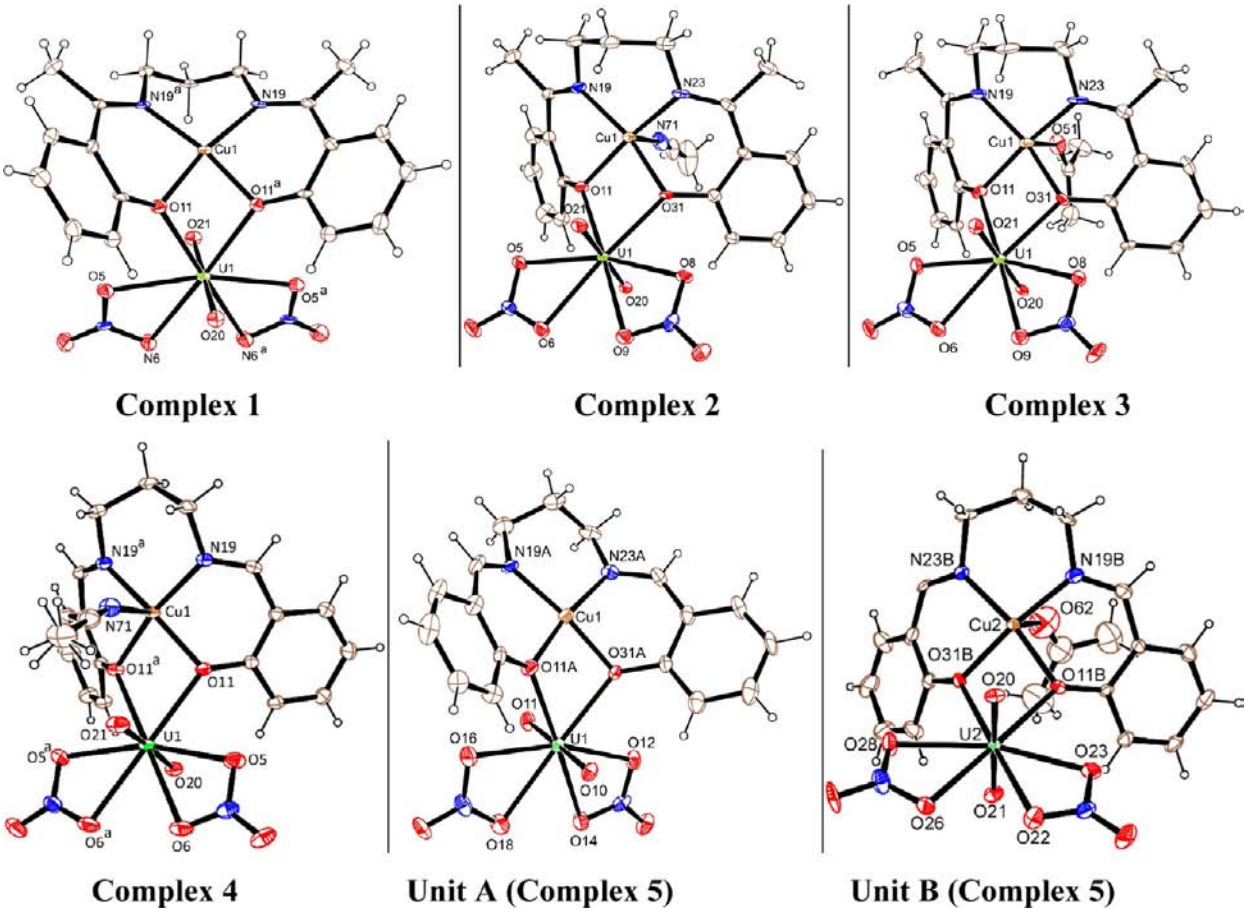

Figure 4. ORTEP diagrams of complexes **1**−**5**. Two other units of **5**, which are equivalent to units A and B, are shown in Supporting Information, Figure S4. Ellipsoids are drawn at the 20% probability level.

spectral properties of the fluorophore and consequently the formation of any emissive complex, for example, uranyl Schiff base complex[34] or exciplex is discarded.[35] The Stern−Volmer (S−V) plots for steady-state fluorescence quenching obtained by using the experimentally determined values of I_0 and I are found to be nonlinear with positive deviation (Figure 2E and 2F). This aspect of the plots suggests the presence of both dynamic and static quenching. Therefore the data are analyzed by the modified Stern−Volmer equation for static and dynamic quenching (eq 1 and eq 2), in which the normalized fluorescence intensity (I_0/I) is a function of both static (K_g) and dynamic quenching (K_D) terms:

$$(I_0/I) = (1 + K_g[Q])(1 + K_D[Q]) \quad (1)$$

$$\{(I_0/I) - 1\}/[Q] = (K_g + K_D) + K_g \cdot K_D[Q] \quad (2)$$

where K_g and K_D ($K_D = k_q\tau_0$; k_q is the bimolecular quenching rate constant and τ_0 is the excited lifetime of uranyl nitrate in the absence of the quencher) are the Stern−Volmer constants for static and dynamic quenching, respectively, and Q is the quencher (metalloligand) concentration. Equation 2 is valid for a single species undergoing both dynamic and static quenching describing a quadratic dependence upon the quencher concentration and consequently a positive deviation of the graph I_0/I versus [Q]. Hence the linearity of these plots

dx.doi.org/10.1021/ic400422d | Inorg. Chem. 2013, 52, 7508−7523

obtained from the nonlinear S−V plots suggests that static and dynamic quenching model is well applicable for this system (Figure 2E inset and 2F inset).[36]

Evidence for dynamic quenching of uranyl fluorescence was obtained from time-resolved fluorescence spectroscopy where the average lifetime of excited uranyl decreased with increasing concentration of the individual metalloligands (Figure 2C and 2D). Linear Stern−Volmer plots (Figure 2E and 2F) for dynamic quenching were obtained for both the quenchers from lifetime (τ) measurements according to the eq 3,

$$(\tau_0/\tau) = 1 + K_D[Q] \quad (3)$$

Where τ_0 and τ refer to the lifetime of the excited uranyl ion in the absence and presence of the quencher, respectively. The linearity of the S−V plots for dynamic quenching as well as the fitting of the lifetime decay profiles with biexponential functions for both the quenchers (see χ^2 values in Supporting Information, Tables S5 and S6) indicates dynamic quenching of the excited state lifetime of the fluorophore. Also from the S−V plots (Figure 2E and 2F) it is evident that the slope obtained from the steady-state fluorescence quenching experiment (K_{SV}) is much higher than the slope obtained from time-resolved fluorescence quenching experiment (K_D) (Supporting Information, Table S7) indicating the presence of both static and dynamic quenching.[37] From the above experimental results, static quenching constants (K_g) can be derived from eq 4,[38]

$$(I_0/I)\times(\tau/\tau_0) = (1 + K_g[Q]) \quad (4)$$

The K_g values are thus obtained from the plots (Figure 3A and 3B) for both the metalloligands. Although the values are much higher compared to the association constants (K_a) determined from the UV−vis analysis of CT complex formation between uranyl nitrate and metalloligands (Supporting Information, Table S7), but both experiments indicate the formation of a stable Cu−UO_2 heteronuclear core in solution with moderate formation constants for both the metalloligands in acetonitrile. The accessibility of fluoroprobe to the individual quencher (metalloligands) in acetonitrile has been calculated using eq 5,

$$(I_0/\Delta I) = 1/f_a + 1/K_S f_a[Q] \quad (5)$$

Where $\Delta I = I_0 - I$, K_S = corresponding Stern−Volmer constant, and f_a = fraction of the fluorophore which is accessible to the quencher ([CuL^1] or [CuL^2]). The plots with good linearity have been obtained for both the metalloligands (Figure 3C). The profiles of the fraction of fluoroprobe to the individual metalloligand quencher are 1.1 and 1.2 corroborating the formation of 1:1 Cu−UO_2 heterodinuclear core in acetonitrile.

For the heterometallic TM−UO_2^{2+} complexes (TM = transition metal), deduction of the mechanism of quenching needs rigorous theoretical and experimental analyses. At room temperature the oxidation potentials of ground state square planar Cu^{2+} complexes are in the region of +0.8 to +1.0 V but that of photoexcited $UO_2(NO_3)_2$ reaches a value of about +2.6 V[39] favoring photo induced electron transfer.[40] However, the fluorescence band of uranyl nitrate at higher wavelength region (445−630 nm) merged on the d-d transition bands of the respective complexes (550−800 nm) suggesting the possibility of quenching through energy transfer.[41] Moreover the phenyl rings of the metalloligands may also play important role as they are known to be responsible for dynamic quenching of excited UO_2^{2+}.[31b,42]

Structure Description of the Complexes. The structures of all complexes **1**−**5** (Figure 4 and Supporting Information, Figure S4) contain a heterodinuclear core Cu−UO_2 formed by the coordination of the two phenoxido oxygens of the "metalloligand", [CuL], to the uranyl group. In complex **1**, a mirror plane which passes through the Cu and U atoms bisects the complex. The copper atom shows a square-planar geometry being coordinated by two phenoxido oxygen atoms O(11) and O(11)^a (symmetry code: $^a = x, 1/2 - y, z$) and the two imine nitrogen atoms N(19) and N(19)^a (Supporting Information, Table S1). The root mean squared (r.m.s.) deviation of the four coordinating atoms from the mean plane passing through them is 0.00 Å because of the mirror plane. The copper atom deviates 0.013(4) Å from this plane. This square-planar geometry is also verified by the so-called τ_4 index that measures the distortion between a perfect tetrahedron ($\tau_4 = 1$) and a perfect square planar geometry ($\tau_4 = 0$) with the formula: $\tau_4 = [360° - (a + b)]/141°$, where "$a$" and "$b$"' (in degrees) are the two largest angles around the central metal in the complex (Supporting Information, Table S2).[43] The τ_4 value for Cu(1) in complex **1** is 0.129, confirming a slightly distorted square planar geometry for this metal center.

The geometry around copper centers in complexes **2** and **3** is square-pyramidal, with four equatorially coordinated atoms are O(11), O(31), N(19), and N(23) of the Schiff base and an axially coordinated acetonitrile (in **2**) or acetone (in **3**) solvent molecules at distances 2.342(6) and 2.409(11) Å, respectively. The Cu-phenoxido and Cu-imine bond distances lie in the ranges of 1.945(4)−1.965(9) Å and 1.966(13)−1.991(6) Å respectively (Supporting Information, Table S1). The r.m.s. deviation of the four basal atoms from the mean plane for complex **2** is 0.015 Å with the metal atom 0.187(1) Å from this plane toward the axially coordinated nitrogen atom N(71). The same deviation for complex **3** is 0.025 with the metal atoms 0.164(2) Å from the plane toward the coordinated solvent molecule. The Addison parameter of Cu(1) atom in the complexes **2** and **3** are 0.031 and 0.041 respectively; indicating negligible amount of distortion toward trigonal bipyramid geometry.[44] Complex **4** contains a plane of symmetry perpendicular to the crystallographic b axis passing through the Cu and U atoms like **1**. However, unlike **1** the geometry around the copper center in **4** is square-pyramidal being coordinated equatorially by two phenoxido oxygen atoms O(11) and O(11)^a (symmetry code: $^a = x, 1/2 - y, z$) and the two imine nitrogen atoms N(19) and N(19)^a (Supporting Information, Table S1) with axially coordinated acetonitrile molecules at a distance of 2.415(7) Å. The metal atom deviates 0.215(2) Å from the mean plane passing through the four coordinating atoms toward the axially coordinated nitrogen atom N(71).

Complex **5** consists of four asymmetric dinuclear Cu(UO_2) units, namely, A, B, C, and D. The structures of the units A and C are equivalent having the same molecular formula [{CuL^2}-$UO_2(NO_3)_2$], with some differences in bond angles and distances. Similarly units B and D are equivalent with the formula [{$CuL^2(CH_3COCH_3)$}$UO_2(NO_3)_2$]. The structures of units A and B are shown in Figure 4 together with the atomic numbering scheme whereas the same for units C and D are shown in the Supporting Information, Figure S4. The copper atoms in each heterodinuclear unit (Cu(1), Cu(2), Cu(3), and Cu(4) respectively) are coordinated by two phenoxido oxygen

dx.doi.org/10.1021/ic400422d | Inorg. Chem. 2013, 52, 7508−7523

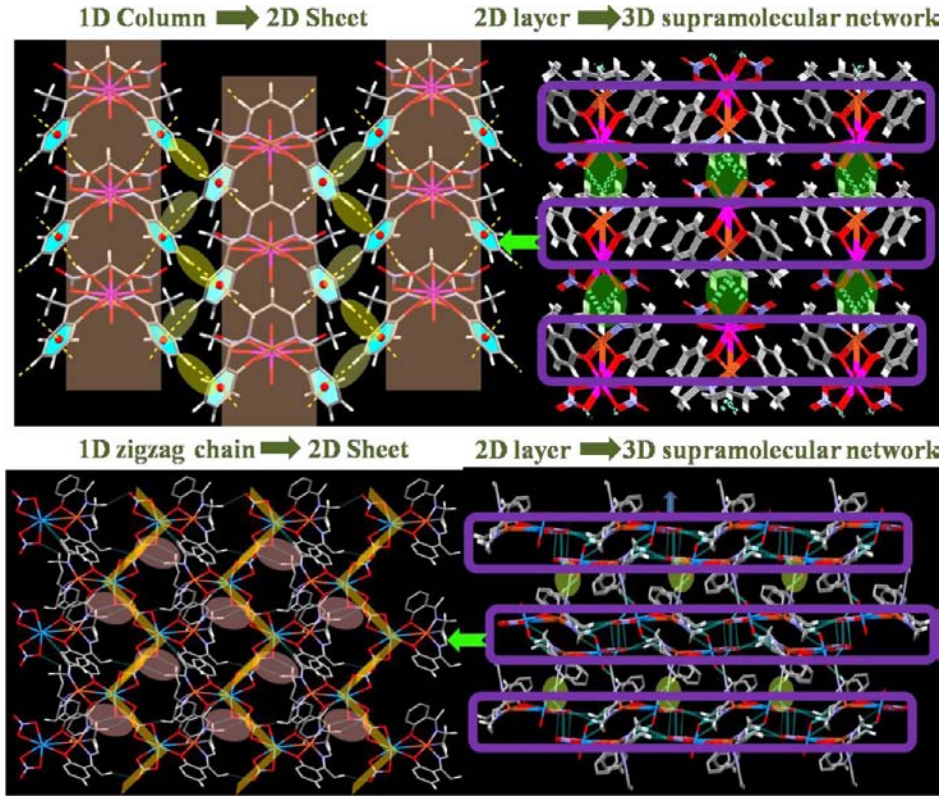

Figure 5. Upper panel shows the 3D-supramolecular interactions of complex **1** and Lower panel shows the 3D-supramolecular interactions of complex **2**. Left panel shows assembly of 1D Chain to form 2D Sheets (viewed through *bc* plane and *ab* plane for complexes **1** and **2** respectively), and Right panel shows mutual interaction of each 2D layer to form 3D supramolecular architecture (viewed through *c* axis and *b* axis for complexes **1** and **2** respectively).

atoms and two imine nitrogen atoms from the Schiff base forming a basal plane as in complexes **1**−**4**. These bond distances are in the range of 1.935(12)−1.960(10) Å for phenoxido oxygen atoms and 1.944(14)−1.968(16) Å for imine nitrogen atoms. Among the four copper atoms, Cu(2) and Cu(4) in units B and D show a square pyramidal geometry with axially coordinated acetone molecules at a distance of 2.73(3) and 2.572(19) Å, respectively (Supporting Information, Table S3). Cu(1) in unit A shows a square planar geometry (τ_4 = 0.118); the r.m.s. deviation of the four basal atoms from the mean plane is 0.046 Å with the copper atom only at 0.022(2) Å from this plane. The nearest nonbonded O(29) of a nitrato ion is at 3.257(17) Å from the Cu(II) indicating no ancillary interactions between them. Cu(3) in unit C also shows a square planar geometry but with an ancillary interaction at the distance of 2.822(15) Å with the oxygen atom O(49) of the nitrato ligand of the unit D. These kinds of ancillary interactions also take place between O(15) and O(39) of the nitrato ligands of units A and C and Cu(2) and Cu(4) of units B and D with slightly longer distances of 2.912(19) and 2.905(19) Å, respectively. The deviation of the copper atoms from the mean N_2O_2 basal plane seems to be a good indicator of axial interactions. This deviation is the highest (0.114(2) Å toward O(49) of the nitrato ligand for Cu(3)) in which the axial interaction is only from one side but is considerably less (0.035(2) and 0.027(2) Å for Cu(2) and Cu(4) respectively) in units B and D where axial bonds or ancillary interactions are from both sides of the equatorial plane. The τ_4 value for Cu(3) is 0.145 confirming slight tetrahedral distortion for this metal center. The Addison parameters of Cu(2) and Cu(4) are 0.061 and 0.007, respectively, indicating that these metal centers have negligible amount of distortion toward trigonal bipyramidal geometry.

One of the important structural variations among complexes **1**−**5** is the different coordination numbers and modes in the copper center due to change of the Schiff base which adopt a "boat-like" conformation making the shape of the complexes as a "bowl". In case of complex **4** the solvent molecule (acetonitrile) coordinates to the copper center along the convex part of the bowl whereas for complexes **2**, **3**, and **5** the solvent molecules (acetonitrile, acetone, and acetone, respectively) coordinate along the concave part (Figure 4 and Supporting Information, Figure S4).

The uranium atom in all five complexes (**1**−**5**) adopts an octa-coordinated UO_8 environment with distorted hexagonal bipyramidal geometry. The axial positions are occupied by the oxygen atoms of uranyl ion with short U−O distances in the range 1.727(11)−1.767(4) Å (Supporting Information, Tables S1 and S3) which are typical of the double uranyl bond, commonly found for hexavalent uranium.[45] The trans OUO angles (Supporting Information, Tables S2 and S4) which are in the range 179.4(2)°−176.2(4)° show slight deviation from linearity. Two of the six oxygen atoms in the equatorial plane belong to the phenoxido oxygen atoms of the metalloligands, and the other four oxygen atoms to two nitrato coligands that coordinate as chelated bidentate ligands. The U-phenoxido and U-nitrato bond distances of all five complexes are in the ranges of 2.386(18)−2.446(11) Å and 2.450(11)−2.548(12) Å, respectively (Supporting Information, Tables S1 and S3). The chelating angles to the uranyl center by the metalloligands lie in

dx.doi.org/10.1021/ic400422d | *Inorg. Chem.* 2013, 52, 7508−7523

Table 2. C−H···π Interaction for Complexes 1, 4, and 5

interaction	atoms	distances H···C_g (Å)	∠ C−H···C_g (deg)	distances C(H)···C_g (Å)	symmetry code
		Complex **1**			
C−H···π (side chain)	C(9)−H(9B)···C_g(5)	3.20	130	3.90	*x*,*y*,−1+*z*
C−H···π (phenyl)	C(4)−H(4)···C_g(5)	3.04	132	3.73	*x*,*y*,−1+*z*
		Complex **4**			
C−H···π (methyl)	C(62)−H(62C)···C_g(4)	3.11	158	4.01	−1+*x*,*y*,*z*
		Complex **5**			
C−H···π (methyl)	C(53)−H(53C)···C_g(17)	3.10	122	3.71	*x*,*y*,*z*
	C(63)−H(63C)···C_g(8)	3.08	136	3.83	*x*,*y*,*z*

the range of 62.2(3)°−64.6(3)° whereas those of nitrato ligands are in the range of 49.5(4)°−51.3(2)° (Supporting Information, Tables S2 and S4). The UO_8 coordination polyhedron shares an edge with the Cu coordination polyhedron through the phenoxido oxygen atoms where the Cu−U distance lies in the range of 3.422(1)−3.429(1) Å for complexes **2**−**4** whereas the same for complex **1** is 3.276(4) Å. However the Cu−U distances (3.365(2)−3.400(2) Å) in all units of complex **5** are slightly lower than those for complexes **2**, **3**, and **4** but are higher than that in complex **1**.

The packing of the molecules in complex **1** is controlled by C−H···π and C−H···O interactions. There are two types of C−H···π interactions, namely, C−H···π (side chain) and C−H···π (phenyl), between the neighboring molecules to generate a two-dimensional (2D) supramolecular network (Figure 5 upper panel). In the first case two C−H···π interactions are established between the hydrogen atoms H(9B) of the side chain of methylene group and the phenyl rings of the Schiff base forming a one-dimensional (1D) column where the distance between H(9B) and the centroid of the ring is 3.20 Å and the C(9)−H(9B)···Cg angle is 130° [Cg = centroid of the phenyl ring]. Further, these columns interact with each other through C−H···π (phenyl) interactions where the aromatic hydrogen atom H(4) interacts with the phenyl group of the adjacent molecule forming a 2D sheet. The distance between H(4) and the centroid of the ring is 3.04 Å and the C(4)−H(4)···Cg angle is 132°. The oxygen atoms of nitrato coligands and uranyl moiety also take part in C−H···O hydrogen bonding with different types of C−H bonds which ultimately leads to the three-dimensional (3D)-supramolecular architecture (Figure 5 upper panel; Table 2 and 3).

The packing of the molecules in complexes **2** and **3** is controlled by NO_3^-···NO_3^- interactions and C−H···O hydrogen bonds. For complexes **2** and **3** the nitrato coligands from adjacent molecular units interact mutually in antiparallel fashion[46] forming an infinite 1-D zigzag chain (Figure 5 lower panel and Supporting Information, Figure S5). The N···O distances of complexes **2** and **3** lie in the range of 2.929(19)−3.012(10) Å. In complex **4** the N···O distances are relatively long (3.078(6) Å) indicating weaker interaction compared to complexes **2** and **3** (Table 4). Detailed analyses of these interactions are done in the theoretical part. The oxygen atoms of nitrato coligands and uranyl moiety also take part in unconventional C−H···O hydrogen bonding with different types of C−H bonds which ultimately leads to the 3D-supramolecular architecture (Table 3) for all three complexes. However, weak C−H···π and π···π interactions have also been found in complex **4** (Supporting Information, Figure S6, Tables 2 and 5).

Unlike complexes **1**−**4**, complex **5** shows a different molecular arrangement with uncommon U═O···NO_3^- and

Table 3. C−H···O Interaction for Complexes 1−5

atoms	distances H···O (Å)	∠ C−H···O (deg)	distances C(H)···O (Å)	symmetry code
	Complex **1**			
C(3)−H(3)···O(5)	2.74	140	3.51	*x*,*y*,1+*z*
	Complex **2**			
C(12)−H(12C)···O(7)	2.56	148	3.41(1)	−1+*x*,*y*,*z*
C(16)−H(16)···O(20)	2.40	168	3.32(1)	−1/2+*x*,1/2−*y*,1−*z*
	Complex **3**			
C(16)−H(16)···O(20)	2.45	159	3.34	−1/2+*x*,1/2−*y*,−*z*
C(22)−H(22B)···O(10)	2.59	149	3.52	−1/2+*x*,3/2−*y*,−*z*
	Complex **4**			
C(62)−H(62B)···O(6)	2.72	154	3.60	*x*,1/2−*y*,−1+*z*

NO_3^-···NO_3^- interactions. The U═O···NO_3^- interactions take place between two adjacent units, namely, units A and B and units C and D, to form two self-assembled dimers (Supporting Information, Figure S7). The distances between the interacting atoms, that is, oxygen atom of the uranyl moiety and nitrogen atom of the nitrato coligand, lie in the range of 2.84(3)−3.00(3) Å, and the U═O···N angles are in the range of 133.6(7)°−138.9(6)°. These self-assembled dimers further interact through U═O···NO_3^- and NO_3^-···NO_3^-. The distances and angles of the U═O···N interaction are 2.86(2) Å and 133.2(6)° whereas those of the N═O···N interactions are 3.07(3) Å and 120.4(14)°, respectively (Table 6). Unlike complex **3**, the coordinated acetone molecules at Cu(2) and Cu(4) atoms of complex **5** are leaning toward one of the phenyl rings of the Schiff base probably because of the weak C−H···π interaction between the hydrogen atoms H(53C) and H(63C) of the methyl group of the two acetone molecules (Supporting Information, Figure S7). The distances between H(53C) and H(63C) and the centroids of the rings are 3.10 and 3.08 Å, and the C−H···Cg angles are 122° and 136° respectively [Cg = centroid of the phenyl ring] (Table 2).

Theoretical Study. As described above, five new structures containing the UO_2^{2+} core have been synthesized and characterized by their X-ray structures, and they present very interesting noncovalent interactions in the solid state. They are U−Cu dinuclear compounds and are represented in Figure 4. The organic ligand is denoted as [L^1] in complexes **1**, **2**, and **3** and denoted as [L^2] in complex **4**. Complex **1** does not present any solvent molecule coordinated to the Cu atom. Complexes **2** and **4** present an acetonitrile molecule coordinated to the Cu atom. Interestingly, it is coordinated to the concave part of the

dx.doi.org/10.1021/ic400422d | Inorg. Chem. 2013, 52, 7508−7523

Table 4. $NO_3^-\cdots NO_3^-$ Interaction for Complexes 2, 3, and 4[a]

measure	atoms	complex 2	complex 3	complex 4
distances (Å)	N(4)−O(7)′	3.01(1)	2.93(2)	
	N(3)−O(10)′/O(10)″/O(7a)‴	3.01(1)	2.97(2)	3.08(1)
	N(4)−O(10)	1.22(1)	1.22(2)	
	N(3)−O(7)	1.20(1)	1.19(2)	1.19(1)
angles (deg)	O(7)−N(3)−O(10)′/O(10)″ /O(7a)‴	83.7(5)	82.8(10)	70.1(3)
	O(7)′−N(4)−O(10)	83.6(4)	84.5(9)	
	N(3)−O(7)−N(4)′/N(3a)‴	96.1(5)	97.3(10)	109.9(3)
	N(3)′−O(10)−N(4)	95.6(4)	94.6(10)	

[a]Symmetry element ′=1−*x*,−1/2+*y*,1/2−*z* (for **2**) and 2−*x*,1/2+*y*,1/2−*z* (for **3**); ″= 2−*x*, −1/2+*y*,1/2−*z* (for **3**); ‴=−*x*,−*y*,−*z* (for **4**).

Table 5. $\pi\cdots\pi$ Interaction in Complex 4

ring (i) → ring (j)	dihedral and slip angles (i, j) (deg)	centroid (i) to ring (j) distance (Å)	distances between ring centroids (i, j) (Å)	symmetry code
R(4)→ R′(4)	0.00, 48.48	3.265	4.926(3)	1−*x*,− *y*,1−*z*

molecule in **2**, where the ligand is methylated [L^1] and, conversely, to the convex part in complex **4** (nonmethylated ligand, [L^2]). This issue is further analyzed below. In complex **3** the coordinated solvent molecule is acetone, and the geometry resembles complex **2**. In complex **5**, four symmetrically different dinuclear complexes (A−D) are present in the solid state (bottom right part of Figure 4 and Supporting Information, Figure S4). Two of them (A and C) do not have a solvent molecule coordinated and the other ones (B and D) have an acetone solvent molecule coordinated to the copper metal center.

The theoretical study has been performed using DFT calculations including the latest correction for dispersion developed by Grimme (D3). The level of theory is BP86-D3/def2-TZVP (for U the basis set is def2-TZVPP). Using this level we have evaluated some interesting noncovalent interactions observed in the solid state. We have analyzed the different behavior of the complexes depending on the presence or absence of a solvent molecule coordinated to the concave part of the dinuclear complex. In complexes **2** and **3** an unexpected and short $NO_3^-\cdots NO_3^-$ interaction is observed. This interaction is relevant since it greatly influences the crystal packing (Figure 6). Intuitively it should be repulsive because of significant charge repulsion. However, since the nitrate anions are coordinated to the uranium metal center, most of the negative charge is transferred to the metal. In fact, we have calculated the $NO_3^-\cdots NO_3^-$interaction in a neutral model, that is, $UO_2(NO_3)_2$, and the computed interaction energy is favorable (−2.8 kcal/mol). However, the real system is a dinuclear complex where the presence of additional donating bridging ligands causes a weakening of this interaction that is −0.8 kcal/mol in **2** and −0.4 kcal/mol in **3**. It should be mentioned that the latter energy is close to the limit of the intrinsic error of the theoretical method (<0.5 kcal/mol); therefore, a definite conclusion cannot be extracted from this value. However, the binding energies computed for compound **2** and the neutral model clearly support the stabilizing effect of this interaction.

In complex **1**, the absence of any coordinating solvent molecule allows the formation of a totally different packing, as previously shown in the description of the structures. In fact the aliphatic chain that connects the nitrogen atoms of the ligand occupies this cavity, generating a more compact packing (Figure 7). As a consequence an infinite column is generated where a combination of C−H/π and hydrogen bonding interactions are established. The hydrogen atoms of the aliphatic chain participate in the C−H/π interactions, and the hydrogen bonds are formed between the coordinated nitrate anions and the aromatic hydrogen atoms. Since the nitrate ligands participate in these hydrogen bonds (among others, vide supra), they are not available to establish the $NO_3^-\cdots NO_3^-$ interactions observed in complexes **2** and **3**. As a matter of fact, in those complexes the presence of the coordinated solvent molecule prevents the formation of these compact infinite columns. We have computed the interaction energy of a dimer (Figure 8), which is −18.6 kcal/mol that corresponds to two C−H/π and two hydrogen bonding interactions. To know the contribution of each interaction, we have computed a model where the aliphatic chain has been replaced by two hydrogen atoms in one molecule (Figure 7, bottom right). Thus, in this model the C−H/π interactions are not present. The interaction energy is reduced from −18.6 to −10.8 kcal/mol, which corresponds to the strength of the hydrogen bonds. Thus, the interaction energy of both C−H/π interactions is approximately −7.8 kcal/mol. It should be mentioned that this is a rough estimation since the structural consequence of replacing the methylene group by a hydrogen atom is not taken into account.

Table 6. U═O$\cdots NO_3^-$ and $NO_3^-\cdots NO_3^-$ Interactions for Complex 5

units	O···N atoms	distances (Å)	N−O···N atoms	angles (deg)
A and B	O(11)···N(27)	3.00(3)	U(1)−O(11)···N(27)	138.9(6)
	O(20)···N(13)	2.87(3)	U(2)−O(20)···N(13)	137.3(7)
C and D	O(31)···N(47)	2.84(3)	U(3)−O(31)···N(47)	134.8(7)
	O(40)···N(37)	2.93(2)	U(4)−O(40)···N(37)	133.6(7)
B and C	O(21)···N(33)	2.86(2)	U(2)−O(21)···N(33)	133.2(6)
	O(35)···N(24)	3.07(3)	N(33)−O(35)···N(24)[a]	120.4(14)

[a]N−O···N for $NO_3^-\cdots NO_3^-$ interaction.

dx.doi.org/10.1021/ic400422d | Inorg. Chem. 2013, 52, 7508−7523

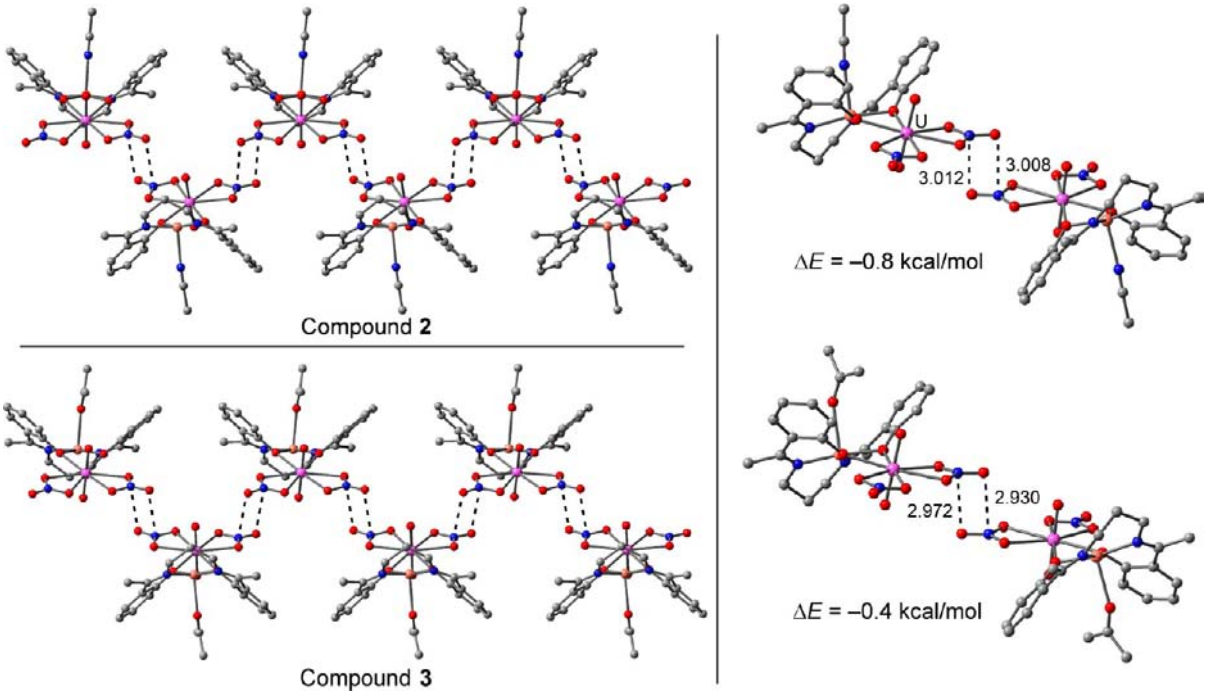

Figure 6. Left: Partial views of the X-ray structure of complexes **2** and **3** with indication of the $NO_3^-\cdots NO_3^-$ interactions. Right: interaction energies associated to the $NO_3^-\cdots NO_3^-$ contacts. Distances in angstrom (Å).

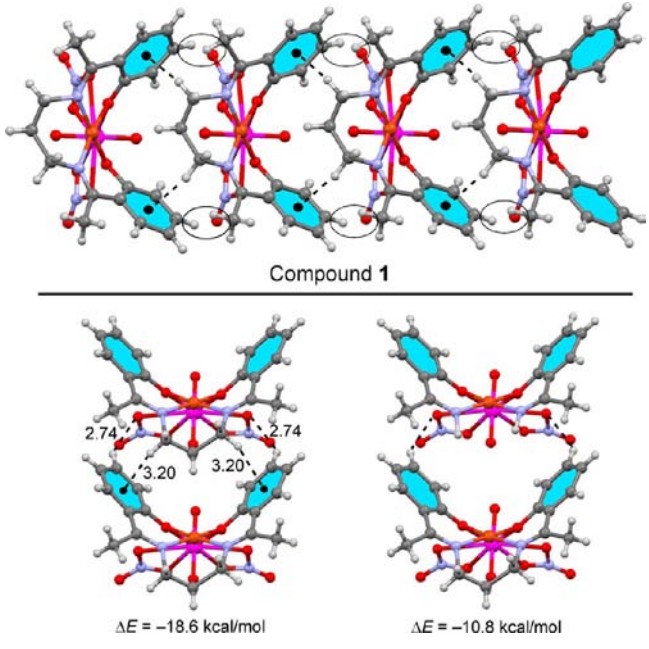

Figure 7. Top: Partial views of the X-ray structure of complex **1** with indication of the C–H/π (dashed lines) and the hydrogen bonding (encircled) interactions. Bottom: Computational models used to estimate the interaction energies associated to the noncovalent contacts. Distances in angstrom (Å).

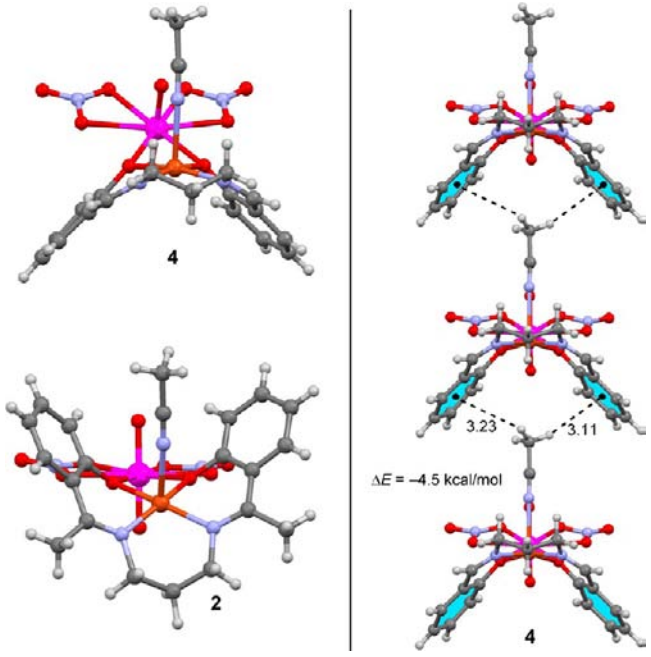

Figure 8. Left: X-ray structures of complexes **2** and **4**. Right: infinite 1D column observed in the crystal packing of **4**.

Complex **4** is characterized by having the solvent molecule coordinated to the convex part of the molecule, in sharp contrast to complexes **2**, **3**, and **5** (Figure 8, left). The concave part has the adequate size and shape to accommodate a methyl group of another molecule for the formation of infinite columns in the crystal structure (Figure 8, right). Interestingly, this 1D column is formed by means of weak C–H/π interactions that have a very relevant role in this structure, even in the presence of strong hydrogen bonds. Each column is surrounded by four columns, two of which in a parallel fashion and two in an antiparallel fashion mostly govern the final 3D architecture of this compound in the solid state. The columns interact with each other by means of C–H···O hydrogen bonds and π–π interactions. The representation of parallel/antiparallel arrangement of the columns in two directions of the crystal packing is represented in Figure 9. We have computed the interaction energy of this double C–H/π interaction, which is −4.5 kcal/mol (Figure 8, right). This interaction is likely enhanced by the

dx.doi.org/10.1021/ic400422d | Inorg. Chem. 2013, 52, 7508–7523

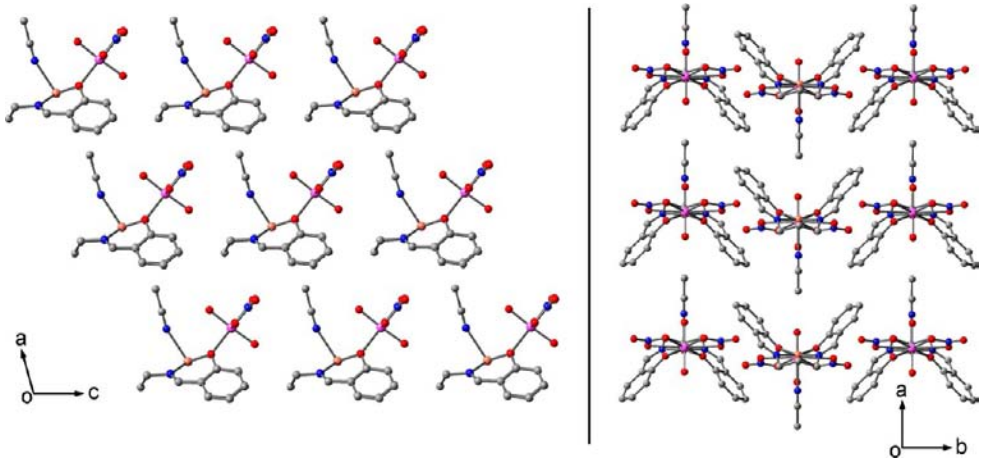

Figure 9. Parallel (left) and antiparallel columns (right) observed in complex **4**. The hydrogen atoms have been omitted for clarity.

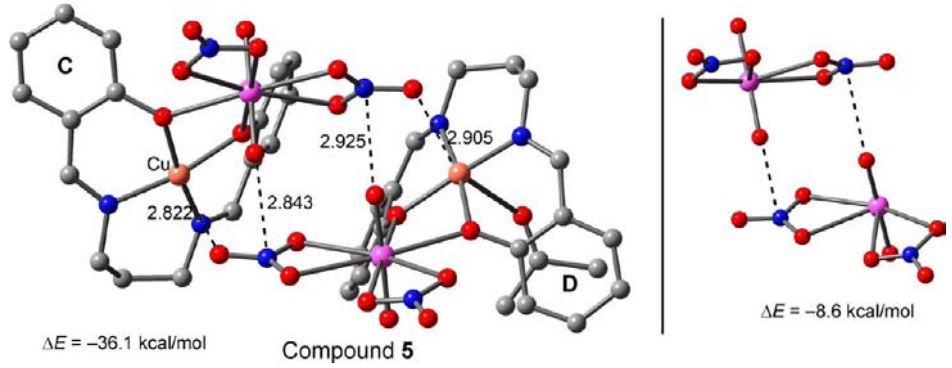

Figure 10. Left: Partial view of the X-ray structure of complex **5**. Distances in angstrom (Å). Right: Theoretical model to evaluate the U═O···NO_3^- interaction.

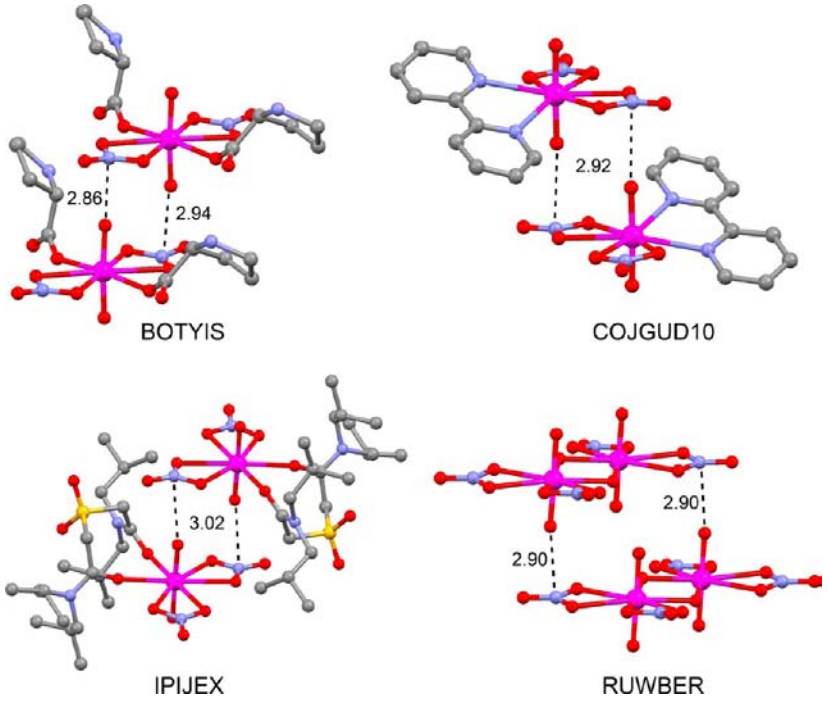

Figure 11. X-ray structures retrieved from the CSD exhibiting U═O···NO_3^- interactions. Distances in angstrom (Å).

coordination of the acetonitrile to the Cu metal center that increases the acidity of the methyl hydrogen atoms.

Finally, for complex **5** we have analyzed a peculiar arrangement of the molecules observed in the solid state

dx.doi.org/10.1021/ic400422d | *Inorg. Chem.* 2013, 52, 7508−7523

forming dimers, where the oxygen atom coordinated to the uranium metal center is pointing to the nitrogen atom of the nitrate anion at a distance shorter than 3.0 Å (Figure 10) and simultaneously the oxygen atom of the nitrate anion is close to the Cu metal center of the other molecule, establishing an ancillary interaction. This self-assembled dimer is stabilized by the formation of one pair of each of the aforementioned interactions. The interaction energy of the dimer is −36.1 kcal/mol. To know the contribution of the uncommon U═O···NO_3^- interaction, we have computed the binding energy of a model dimer where the [CuL^2] part has been removed. The interaction of this model is −8.6 kcal/mol (Figure 10, right), indicating that each U═O···NO_3^- interaction is at least −4.3 kcal/mol. This value is probably underestimated since in the real system the nitrogen atom of the NO_3^- ligand is more electrophilic because of the charge donation to the Cu atom. In any case, for this compound this interesting interaction contributes to the formation of the dimers observed in the solid state, and the O···N distance is similar to the one observed in compounds **2** and **3** where NO_3^-···NO_3^- interactions resembling an antiparallel stacking are formed (Tables 4 and 6). Moreover, the NO_3^-···Cu distance is shorter in the Cu atom that is not coordinated to the solvent molecule, and, consequently, the U═O···NO_3^- distance is also shorter.

As suggested by one referee, we have searched the Cambridge Structural Database (CSD) to investigate if this unusual U═O···NO_3^- interaction is also present in other X-ray structures, to further demonstrate the existence and relevance of this interaction. In the search we have found 12 structures where this interaction is clearly observed and plays a very relevant role in the crystal packing. The full list of structures is included in Supporting Information, Table S9, and we have selected four to illustrate the interactions which are shown in Figure 11. In most cases the U═O···N distances are very short (≈ 3.0 Å) and similar to those observed for compound **5**. In addition, in the structures retrieved from the CSD there are not additional Cu···O interactions as in **5** and consequently the formation of dimers or, in most cases, 1D infinite columns is due to several simultaneous U═O···NO_3^- interactions. The importance of this previously unnoticed interaction should be emphasized since it may have relevance in crystal engineering or supramolecular chemistry fields.

CONCLUDING REMARKS

Five heterobimetallic copper(II)−uranium(VI) complexes have been synthesized by reacting Cu(II)-derived metalloligands with $UO_2(NO_3)_2{\cdot}6H_2O$ in 1:1 ratio by varying the reaction temperature and solvents. Steady-state and time-resolved fluorescence quenching experiments established the formation of a 1:1 ground-state charge transfer copper(II)−uranyl(II) complexes in solution. The photophysical investigation is proved to be a good experimental tool for characterization of heteronuclear Cu(II)−U(VI) complexes in solution and may be further extended to characterize the formation of heterometallic complexes involving U(VI) and metal-chelates which are known to be quenchers of uranyl fluorescence. X-ray single-crystal structure reveals that each complex contains a diphenoxido bridged Cu(II)−U(VI) dinuclear core with two terminally coordinated nitrato coligands. The nitrato coligands are labile and can be replaced by various ligands suggesting the future perspective of applicability of these complexes as heterobimetallic Cu-UO_2 tectons for high nuclearity heterometallic clusters or coordination polymers. These complexes present a variety of solvation modes in the axial position of the Cu(II) that influence the final solid state structure. The absence of coordinated solvent molecules to the concave part of the molecule, as in **1** and **4**, causes the formation of infinite 1D columns, which are stabilized by means of interesting C−H/π interactions either using the aliphatic chain belonging to the ligand (**1**) or the methyl group of the acetonitrile coordinated to the convex part (**4**). In the other complexes the presence of a solvent molecule prevents the formation of these columns and other packing is observed, where uncommon NO_3^-···NO_3^- or U═O···NO_3^- interaction is established, resembling recently described antiparallel and perpendicular carbonyl−carbonyl interactions.[47] Characterization of these various uncommon solid state interactions between NO_3^-···NO_3^- or U═O···NO_3^- may enlighten the solid state properties of $UO_2(NO_3)_2$ clusters which are one of the important precursors in nuclear waste materials.

ASSOCIATED CONTENT

Supporting Information

Crystallographic data in CIF format. Further details are given in Figures S1−S7 and Tables S1−S8. This material is available free of charge via the Internet at http://pubs.acs.org.

AUTHOR INFORMATION

Corresponding Author

*E-mail: toni.frontera@uib.es (A.F.), ghosh_59@yahoo.com (A.G.).

Notes

The authors declare no competing financial interest.

ACKNOWLEDGMENTS

We are thankful to the University Grants Commission (UGC), New Delhi, for the Junior Research Fellowship to S.G. [Sanction no. UGC/748/Jr. Fellow (Sc)], Council of Scientific and Industrial Research (CSIR), New Delhi, for the Senior Research Fellowship to S.B. [Sanction no. 09/028 (0732)/2008-EMR-I], and DST-FIST, India, for the Single Crystal X-ray Diffractometer Facility at the Department of Chemistry, University of Calcutta. This work was supported by the DGICYT of Spain (CTQ2011-27512/BQU and CONSOLIDER INGENIO CSD2010-00065, FEDER funds) and the Direcció General de Recerca i Innovació del Govern Balear (project 23/2011, FEDER funds). We present our sincere gratitude to Prof. Sanjib Ghosh and Mr. Swarna Kamal Samanta, Department of Chemistry and Biochemistry, Presidency University, 86/1, College Street, Kolkata 700073, India, for performing the time-resolved fluorescence spectroscopic studies under the financial support of DST (SR/S1/PC-57/2008) and CSIR (No. 21(0871)/11/EMR-II) and also for their valuable advice throughout the spectroscopic experiments. We also thank Dr. Nikhil Guchhait, Department of Chemistry, University College of Science, University of Calcutta, for the helpful suggestions throughout the steady-state fluorescence spectroscopic investigations.

REFERENCES

(1) (a) Andruh, M. *Chem. Commun.* **2007**, 2565−2577. (b) Mondal, K. C.; Sundt, A.; Lan, Y.; Kostakis, G. E.; Waldmann, O.; Ungur, L.; Chibotaru, L. F.; Anson, C. E.; Powell, A. K. *Angew. Chem., Int. Ed.* **2012**, *51*, 7550−7554. (c) Gao, T.; Xu, L.-L.; Zhang, Q.; Li, G.-M.; Yan, P.-F. *Inorg. Chem. Commun.* **2012**, *26*, 60−63. (d) Peng, J.-B.; Zhang, Q.-C.; Kong, X.-J.; Zheng, Y.-Z.; Ren, Y.-P.; Long, L.-S.;

Huang, R.-B.; Zheng, L.-S.; Zheng, Z. *J. Am. Chem. Soc.* **2012**, *134*, 3314−3317.
(2) (a) Alsobrook, A. N.; Zhan, W.; Albrecht-Schmitt, T. E. *Inorg. Chem.* **2008**, *47*, 5177−5183. (b) Adelani, P. O.; Albrecht-Schmitt, T. E. *Cryst. Growth Des.* **2011**, *11*, 4676−4683. (c) Salmon, L.; Thuéry, P.; Ephritikhine, M. *Polyhedron* **2007**, *26*, 645−652. (d) Nyman, M.; Burns, P. C. *Chem. Soc. Rev.* **2012**, *41*, 7354−7367.
(3) (a) Mazzanti, M. *Nat. Chem.* **2011**, *3*, 426−427. (b) Le Borgne, T.; Rivière, E.; Marrot, J.; Girerd, J.-J.; Ephritikhine, M. *Angew. Chem., Int. Ed.* **2000**, *39*, 1647−1649. (c) Salmon, L.; Thuéry, P.; Rivière, E.; Ephritikhine, M. *Inorg. Chem.* **2006**, *45*, 83−93. (d) Love, J. B. *Chem. Commun.* **2009**, 3154−3165. (e) Arnold, P. L. *Nat. Chem.* **2012**, *4*, 967−969. (f) Mougel, V.; Chatelain, L.; Pécaut, J.; Caciuffo, R.; Colineau, E.; Griveau, J.-C.; Mazzanti, M. *Nat. Chem.* **2012**, *4*, 1011−1017.
(4) (a) Del Nero, M.; Galindo, C.; Barillon, R.; Madé, B. *Environ. Sci. Technol.* **2011**, *45*, 3982−3988. (b) Geissler, A.; Merroun, M.; Geipel, G.; Reuther, H.; Selenska-Pobell, S. *Geobiology* **2009**, *7*, 282−294. (c) Liu, J.; Brown, A. K.; Meng, X.; Cropek, D. M.; Istok, J. D.; Watson, D. B.; Lu, Y. *Proc. Natl. Acad. Sci. U.S.A.* **2007**, *104*, 2056−2061. (d) Sather, A. C.; Berryman, O. B.; Rebek, J. *J. Am. Chem. Soc.* **2010**, *132*, 13572−13574. (e) Hazer, O.; Kartal, S. *Talanta* **2010**, *82*, 1974−1979.
(5) (a) Natrajan, L. S. *Coord. Chem. Rev.* **2012**, *256*, 1583−1603. (b) Michon, J.; Frelon, S.; Garnier, C.; Coppin, F. *J. Fluoresc.* **2010**, *20*, 581−590. (c) Liu, J.; Zhang, T.; Lu, T.; Qu, L.; Zhou, H.; Zhang, Q.; Ji, L. *J. Inorg. Biochem.* **2002**, *91*, 269−276.
(6) (a) Sakamoto, M.; Manseki, K.; Ōkawa, H. *Coord. Chem. Rev.* **2001**, *219*−*221*, 379−414. (b) Yao, M.-X.; Zheng, Q.; Qian, K.; Song, Y.; Gao, S.; Zuo, J.-L. *Chem.—Eur. J.* **2013**, *19*, 294−303. (c) Andruh, M. *Chem. Commun.* **2011**, *47*, 3025−3042.
(7) (a) Novitchi, G.; Shova, S.; Caneschi, A.; Costes, J. P.; Gdaniec, M.; Stanica, N. *Dalton Trans.* **2004**, 1194−1200. (b) Biswas, S.; Ghosh, A. *Polyhedron* **2011**, *30*, 676−681. (c) Das, L. K.; Kadam, R. M.; Bauzá, A.; Frontera, A.; Ghosh, A. *Inorg. Chem.* **2012**, *51*, 12407−12418. (d) Das, L. K.; Park, S.-W.; Cho, S. J.; Ghosh, A. *Dalton Trans.* **2012**, *41*, 11009−11017. (e) Seth, P.; Das, L. K.; Drew, M. G. B.; Ghosh, A. *Eur. J. Inorg. Chem.* **2012**, 2232−2242. (f) Biswas, S.; Diaz, C.; Ghosh, A. *Polyhedron* **2013**, *51*, 96−101. (g) Das, L. K.; Ghosh, A. *Cryst. Eng. Comm.* **2013**, DOI: 10.1039/C3CE40382C.
(8) (a) Biswas, S.; Naiya, S.; Drew, M. G. B.; Estarellas, C.; Frontera, A.; Ghosh, A. *Inorg. Chim. Acta* **2011**, *366*, 219−226. (b) Carbonaro, L.; Isola, M.; La Pegna, P.; Senatore, L.; Marchetti, F. *Inorg.Chem.* **1999**, *38*, 5519−5525. (c) Biswas, S.; Ghosh, A. *Ind. J. Chem, Sec A* **2011**, *50*, 1356−1362. (d) Oz, S.; Arici, C.; Emregul, K. C.; Ergun, Ü.; Atakol, O.; Kenar, A. *Z. Kristallogr.* **2007**, *222*, 249−254. (e) Thurston, J. H.; Ely, T. O.; Trahan, D.; Whitmire, K. H. *Chem. Mater.* **2003**, *15*, 4407−4416. (f) Biswas, S.; Naiya, S.; Gómez-García, C. J.; Ghosh, A. *Dalton Trans.* **2012**, *41*, 462−473. (g) Das, L. K.; Drew, M. G. B.; Ghosh, A. *Inorg. Chim. Acta* **2013**, *394*, 247−254. (h) Biswas, S.; Saha, R.; Ghosh, A. *Organometallics* **2012**, *31*, 3844−3850. (i) Bencini, A.; Benelli, C.; Caneschi, A.; Carlin, R. L.; Dei, A.; Gatteschi, D. *J. Am. Chem. Soc.* **1985**, *107*, 8128−8136.
(9) (a) Takao, K.; Kato, M.; Takao, S.; Nagasawa, A.; Bernhard, G.; Hennig, C.; Ikeda, Y. *Inorg. Chem.* **2010**, *49*, 2349−2359. (b) Berthet, J.-C.; Thuéry, P.; Dognon, J.-P.; Guillaneux, D.; Ephritikhine, M. *Inorg. Chem.* **2008**, *47*, 6850−6862. (c) Charushnikova, I. A.; Den Auwer, C. *Russ. J. Coord. Chem.* **2007**, *33*, 53−60. (d) Zucchi, G.; Maury, O.; Thuéry, P.; Gumy, F.; Bünzli, J.-C. G.; Ephritikhine, M. *Chem.—Eur. J* **2009**, *15*, 9686−9696.
(10) (a) Sánchez Mirón, A.; Molina Grima, E.; Fernández Sevilla, J. M.; Chisti, Y.; García Camacho, F. *J. Appl. Phycol.* **2000**, *12*, 385−394. (b) Hosseini, M.; Ganjali, M. R.; Veismohammadi, B.; Faridbod, F.; Abkenar, S. D.; Salavati-Niasari, M. *Luminescence* **2012**, *27*, 341−345. (c) Wernette, D. P.; Mead, C.; Bohn, P. W.; Lu, Y. *Langmuir* **2007**, *23*, 9513−9521.
(11) (a) Fan, L.-J.; Zhang, Y.; Murphy, C. B.; Angell, S. E.; Parker, M. F. L.; Flynn, B. R.; Jones, W. E., Jr. *Coord. Chem. Rev.* **2009**, *253*, 410−422. (b) Fabbrizzi, L.; Licchelli, M.; Pallavicini, P.; Sacchi, D.; Taglietti, A. *Analyst* **1996**, *121*, 1763−1768.
(12) (a) Burrows, H. D.; Pedrosa De Jesus, J. D. *J. Photochem.* **1976**, *5*, 265−275. (b) Burrows, H. D.; Formosinho, S. J.; Miguel, M. D. G.; Coe1ho, F. P. *J. Chem. Soc., Faraday Trans.* **1976**, *72*, 163−171.
(13) (a) Huang, H.; Chaudhary, S.; Van Horn, J. D. *Inorg. Chem.* **2005**, *44*, 813−815. (b) Geipel, G.; Acker, M.; Vulpius, D.; Bernhard, G.; Nitsche, H.; Fanghänel, Th. *Spectrochim. Acta, Part A* **2004**, *60*, 417−424. (c) Sladkov, V.; Fourest, B.; Mercier, F. *Dalton Trans.* **2009**, 7734−7740.
(14) (a) Drew, M. G. B.; Prasad, R. N.; Sharma, R. P. *Acta Crystallogr., Sect. C* **1985**, *41*, 1755−1758. (b) Iida, K.; Oonishi, I.; Nakahara, A.; Komiyama, Y. *Bull. Chem. Soc. Jpn.* **1970**, *43*, 2347−2354. (c) Das, L. K.; Biswas, A.; Frontera, A.; Ghosh, A. *Polyhedron* **2013**, *52*, 1416−1424. (d) Biswas, S.; Ghosh, A. *J. Mol. Struct.* **2012**, *1019*, 32−36.
(15) Bevington, P. R. *Data Reduction and Error Analysis for the Physical Sciences*; McGraw Hill: New York, 1969.
(16) *SAINT*, version 6.02; *SADABS*, version 2.03; Bruker AXS, Inc.: Madison, WI, 2002.
(17) Sheldrick, G. M. *SHELXS 97, Program for Structure Solution*; University of Göttingen: Göttingen, Germany, 1997.
(18) Sheldrick, G. M. *SHELXL 97, Program for Crystal Structure Refinement*; University of Göttingen: Göttingen, Germany, 1997.
(19) Spek, A. L. *J. Appl. Crystallogr.* **2003**, *36*, 7−13.
(20) Farrugia, L. J. *J. Appl. Crystallogr.* **1997**, *30*, 565.
(21) Farrugia, L. J. *J. Appl. Crystallogr.* **1999**, *32*, 837−838.
(22) Ahlrichs, R.; Bär, M.; Hacer, M.; Horn, H.; Kömel, C. *Chem. Phys. Lett.* **1989**, *162*, 165.
(23) Boys, S. B.; Bernardy, F. *Mol. Phys.* **1970**, *19*, 553.
(24) Grimme, S.; Antony, J.; Ehrlich, S.; Krieg, H. *J. Chem. Phys.* **2010**, *132*, 154104-1−154104-19.
(25) Bullock, J. I. *J. Inorg. Nucl. Chem.* **1967**, *29*, 2257−2264.
(26) (a) Golcu, A.; Tümer, M.; Demirelli, H.; Wheatley, R. A. *Inorg. Chim. Acta* **2005**, *358*, 1785−1797. (b) Tümer, M. *Synth. React. Inorg. Met.-Org. Chem.* **2000**, *30*, 1139−1158. (c) Biswas, S.; Ghosh, A. *Polyhedron* **2012**, *39*, 31−37. (d) Biswas, S.; Naiya, S.; Drew, M. G. B.; Ghosh, A. *Indian Chem. Soc.* **2012**, *89*, 1317−1322.
(27) De Costa, M. D. P.; Jayasinghe, W. A. P. A. *J. Photochem. Photobiol., A* **2004**, *162*, 591−598.
(28) (a) Benesi, H. A.; Hildebrand, J. H. *J. Am. Chem. Soc.* **1949**, *71*, 2703−2707. (b) Roberts, E. L.; Chou, P. T.; Alexander, T. A.; Agbaria, R. A.; Warner, I. M. *J. Phys. Chem.* **1995**, *99*, 5431−5437. (c) Hoenigman, S. M.; Evans, C. E. *Anal. Chem.* **1996**, *68*, 3274−3276.
(29) (a) Evans, D. J.; Junk, P. C.; Smith, M. K. *Polyhedron* **2002**, *21*, 2421−2431. (b) Hardwick, H. C.; Royal, D. S.; Helliwell, M.; Pope, S. J. A.; Ashton, L.; Goodacre, R.; Sharrad, C. A. *Dalton Trans.* **2011**, *40*, 5939−5952.
(30) Xie, Y. R.; Zhao, H.; Wang, X. S.; Qu, Z. R.; Xiong, R. G.; Xue, X. X. Z.; You, X. Z. *Eur. J. Inorg. Chem.* **2003**, 3712−3715.
(31) (a) Darmanyan, A. P.; Khudyakov, I. V. *Photochem. Photobiol.* **1990**, *52*, 293−298. (b) Massad, W. A.; Repossi, P.; Argüello, G. A. *J. Colloid Interface Sci.* **2002**, *255*, 189−194. (c) Fonseca, S. M.; Burrows, H. D.; Miguel, M. G.; Sarakha, M.; Bolte, M. *Photochem. Photobiol. Sci.* **2004**, *3*, 317−321.
(32) Kazakov, V. P.; Ostakhov, S. S.; Alyab'ev, A. S.; Osina, I. O. *High Energy Chem.* **2006**, *40*, 248−251.
(33) (a) Burrows, H. D.; Cardosa, A. C.; Formosinho, S. J.; Da Graçia M. Miguel, M. *J. Chem. Soc., Faraday Trans. 1* **1985**, *81*, 49−60. (b) Marcantonatos, M. D. *J. Chem. Soc., Faraday Trans. 1* **1979**, *75*, 2252−2272. (c) Bignozzi, C. A.; Roffia, S.; Scandola, F. *J. Am. Chem. Soc.* **1985**, *107*, 1644−1651.
(34) (a) Vaughn, A. E.; Bassil, D. B.; Barnes, C. L.; Tucker, S. A.; Duval, P. B. *J. Am. Chem. Soc.* **2006**, *128*, 10656−10657. (b) Brancatelli, G.; Pappalardo, A.; Trusso Sfrazzetto, G.; Notti, A.; Geremia, S. *Inorg. Chim. Acta* **2013**, *396*, 25−29. (c) Cozaciuc, I. A.; Postolachi, R.; Gradinaru, R.; Pui, A. *J. Coord. Chem.* **2012**, *65*, 2170−2181.

(35) Evale, B. G.; Hanagodimath, S. M. *J. Lumin.* **2010**, *130*, 1330−1337.
(36) Saha Sardar, P.; Samanta, S.; Maity, S. S.; Dasgupta, S.; Ghosh, S. *J. Phys. Chem. B* **2008**, *112*, 3451−3461.
(37) Repossi, P.; Massad, W. A.; Arguello, G. A. *J. Radioanal. Nucl. Chem.* **2005**, *265*, 85−90.
(38) Timpe, H.-J.; Israel, G.; Becker, H. G. O.; Gould, I. R.; Turro, N. J. *Chem. Phys. Lett.* **1983**, *99*, 275−280.
(39) (a) Rabinowitch, E.; Belford, R. L. *Spectroscopy and Photochemistry of Uranyl Compounds*; Pergamon Press: London, U.K., 1964; (b) Denning, R. G. *J. Phys. Chem. A* **2007**, *111*, 4125−4143. (c) Roundhill, D. M. *Photochemistry and Photophysics of Metal Complexes*; Plenum: New York, 1994.
(40) (a) Burrows, H. D. *Inorg. Chem.* **1990**, *29*, 1549−1554. (b) Katsumura, Y.; Abe, H.; Yotsuyanagi, T.; Ishigure, K. *J. Photochem. Photobiol. A: Chem.* **1989**, *50*, 183−197.
(41) (a) Grohol, D.; Blinn, E. L. *Inorg. Chem.* **1997**, *36*, 3422−3428. (b) Tamilarasan, R.; Ramakrishnan, T.; Endicott, J. F. *Inorg. Chim. Acta* **1987**, *142*, 321−327. (c) Romanovskaya, G. I.; Pogonin, V. I.; Chibisov, A. K. *Zh. Prikl. Spektrosk.* **1980**, *33*, 850−855.
(42) (a) Matsushima, R.; Sakuraba, S. *J. Am. Chem. Soc.* **1971**, *93*, 7143−7145. (b) Matsushima, R. *J. Am. Chem. Soc.* **1972**, *94*, 6010−6016.
(43) Yang, L.; Powell, D. R.; Houser, R. P. *Dalton Trans.* **2007**, 955−964.
(44) Addison, A. W.; Rao, T. N.; Reedijk, J.; Van Rijn, J.; Verschoor, G. C. *J. Chem. Soc., Dalton Trans.* **1984**, 1349−1356.
(45) Pushkin, D. V.; Vologzhanina, A. V.; Serezhkina, L. B.; Savchenkov, A. V.; Korlyukov, A. A.; Serezhkin, V. N. *Russ. J. Inorg. Chem.* **2012**, *57*, 939−944.
(46) (a) Alcock, N. W.; Flanders, D. J. *J. Chem. Soc., Dalton Trans.* **1985**, 1001−1007. (b) Wu, L.; Huang, L.; Shu, M. *Acta Crystallogr. Sect. E* **2012**, *E68*, m422−m423.
(47) Wan, C.-Q.; Mak, T. C. W. *Cryst. Growth Des.* **2011**, *11*, 832−842.

dx.doi.org/10.1021/ic400422d | *Inorg. Chem.* 2013, 52, 7508−7523